2020-02

Fish bladder-based activated porous carbon/co3o4/tio2 composite electrodes for supercapacitors

Sireng, Keith

NM-AIST

FISH BLADDER-BASED ACTIVATED POROUS CARBON/Co_3O_4/TiO_2 COMPOSITE ELECTRODES FOR SUPERCAPACITORS

Keith Sirengo

A Dissertation Submitted in Partial Fulfillment of the Requirements for the Degree of Master's in Materials Science and Engineering at the Nelson Mandela African Institution of Science and Technology

Arusha, Tanzania

February, 2020

ABSTRACT

Supercapacitors as energy storage devices depend on electrode materials, electrolyte and conductive additives. In relation to the above, this master's dissertation specifically provides a scientific understanding and knowledge to the society on the use of fish bladder derived porous carbon for cobalt oxide/titanium dioxide/activated carbon ($Co_3O_4/TiO_2/Ac$) composite as electrode materials for supercapacitor applications. Fish bladder was used as a carbon source for the composite after carbonization and chemical activation. Composites of $Co_3O_4/TiO_2/Ac$, Co_3O_4/Ac, and TiO_2/Ac were later synthesized using simple impregnation method followed by heat treatment and thereafter in-depth investigation on the active material was carried out through material characterization and electrochemical testing. X-ray diffraction and scanning electron microscopy (SEM) revealed that Co_3O_4 and TiO_2 nano phases were well embedded over carbon matrices. Fourier transfer infra-red (FT-IR) measurements showed that the active material had oxygen containing functional groups. Cyclic voltammetry curves demonstrated that specific capacitance of the active material was 946 Fg^{-1} for $Co_3O_4/TiO_2/Ac$ as compared to Co_3O_4/Ac, TiO_2/Ac, and Ac with specific capacitances of 845 F g^{-1}, 340 F g^{-1}, and 308 F g^{-1}, respectively at a scan rate of 5 mVs^{-1}. Impedance spectroscopy revealed good capacitive behavior with a series resistance of 0.5 Ω, 0.52 Ω, 0.6 Ω, and 1.1 Ω for Ac, Co_3O_4/Ac, $Co_3O_4/TiO_2/Ac$, and TiO_2/Ac, respectively. Excellent electrochemical performances observed for the $Co_3O_4/TiO_2/Ac$ electrode was a result of individual contribution of different characteristics of the binary metal oxides such as improved electric conductivity and wettability of the composites associated with porous carbon and TiO_2.

DECLARATION

I, Keith Sirengo, do hereby declare to the Senate of the Nelson Mandela African Institution of Science and Technology that this dissertation is my own original work and that it has neither been submitted nor being concurrently submitted for degree award in any other institution.

_____ _____

Keith Sirengo **Date**

The above declaration is confirmed

_____ _____

Dr. Yusufu Abeid Chande Jande **Date**

_____ _____

Dr. Askwar Hilonga **Date**

_____ _____

Dr. Cecil Kithongo King'ondu **Date**

COPYRIGHT

CERTIFICATION

We hereby confirm that the dissertation entitled "Fish Bladder-Based Activated Porous Carbon/Co_3O_4/TiO_2 Composite Electrodes for Supercapacitors" submitted by Keith Sirengo to the Nelson Mandela African Institution of Science and Technology, Tanzania in partial fulfillment of the requirements for the award of Master's degree in Materials Science and Engineering is an authentic work and has been done under our supervision.

_____ _____

Keith Sirengo **Date**

The above declaration is confirmed

_____ _____

Dr. Yusufu Abeid Chande Jande **Date**

_____ _____

Dr. Askwar Hilonga **Date**

_____ _____

Dr. Cecil Kithongo King'ondu **Date**

ACKNOWLEDGEMENT

My highest gratitude goes to God for giving me life, love, knowledge, and great health for the entire period of my study. Secondly, I pass my regards to my hard working supervisors, Dr. Yusufu Abeid Chande Jande, Dr. Cecil K. Kithongo and Dr. Askwar Hilonga for constant support, significant inputs and fruitful discussions throughout this research journey.

I also wish to thank Dr. Talam Enock for his technical support in my entire research time. Special thanks to the Nelson Mandela African Institution of Science and Technology (NM-AIST) for providing a great learning environment. We greatly appreciate the financial support from Water Infrastructure and Sustainable Energy Futures (WISE-Futures) African centre of excellence. We also appreciate the role played by Botswana International University of Science and Technology and Shinshu University, particularly Prof. Katsuya Teshima of the Center for Energy and Environmental Science in sample characterization.

DEDICATION

My dedication goes to my family, friends and mentors who in one way or the other made this journey a success.

TABLE OF CONTENTS

LIST OF FIGURES

LIST OF ACRONYMS

Acs	Activated carbons
BET	Brunner Emmet Teller
CV	Cyclic Voltammetry
CNT	Carbon Nanotube
EC	Electrochemical capacitor
EDLCs	Electric double layer capacitors
EDS	Energy Dispersive X-ray Spectroscopy
EIS	Electrochemical Impedance Spectroscopy
ESR	Equivalent Series Resistance
FT-IR	Fourier Transform Infrared
GCD	Galvanostatic charge/discharge
KOH	Potassium hydroxide
NMP	N-methyl Pyrrolidone
PANI	Polyaniline
Ppy	Popyrole
PVDF	Polyvinyllideneflouride
Redox	Reduction-oxidation
RGO	Reduced Graphene Oxide
SWCNT	Single Wall Carbon Nanotube

TEM	Transmission Electron Microscope
TMOs	Transition metal oxides
XRD	X-ray diffraction
Z’	Real impedance
Z”	Imaginary impedance
ZIF	Zeoliticimidazolate framework

CHAPTER ONE

INTRODUCTION

1.0 Introduction

This chapter covers the general introduction, objectives, research problems, justifications, hypotheses, and significance of the study. The general objective was to synthesize porous carbon/titanium dioxide/cobalt oxide composites. The general objective was realized through two specific objectives; materials characterization and electrochemical testing of the electrodes.

1.1 Background information

Diminishing rate of fossil fuels accompanied by an alarming rate of environmental pollution as a result of consumption of large quantity of fossil fuel makes it imperative for scientists to move towards sustainable and renewable resources (Cakici *et al.*, 2017). This has lead to a steady shift to renewable energy sources ranging from wind to solar sources of energy as well as a boom in the evolution of hybrid electric dependant vehicles with low carbon dioxide emissions. However, exploitation of these alternative and green energy sources requires efficient storage devices like capacitors, supercapacitors, and batteries that can compensate for their intermittent characteristics (Su *et al.,* 2018). Though their main stumbling block is poor cycle life and low power density, lithium-ion batteries stand out as supreme devices for storage of energy because of the fact that they have high energy density as compared to electrochemical capacitors (Ramesh *et al.*, 2018). This low power density in batteries is due to their low reaction kinetics while their poor cycle life is due to expansion/ contraction that occur between charging and discharging cycles. Contrary to batteries, conventional capacitors have comparatively very low energy density and outstanding power density. Since the current technology demands for storage devices with the capability to meet millions of cycles accompanied by delivery of both first-rate power density and energy density, supercapacitors have shown these properties and therefore may offer a possible option to bridge this existing gap between capacitors and batteries. This, therefore, means that the use of electrochemical capacitors may initiate a scientific leap in energy storage platforms such as industries and

probably address some of the problems that come along with emerging technologies like portable electronics and hybrid vehicles (Jing *et al.*, 2017). Figure 1 shows a Ragone plot of four energy storage and conversion devices.

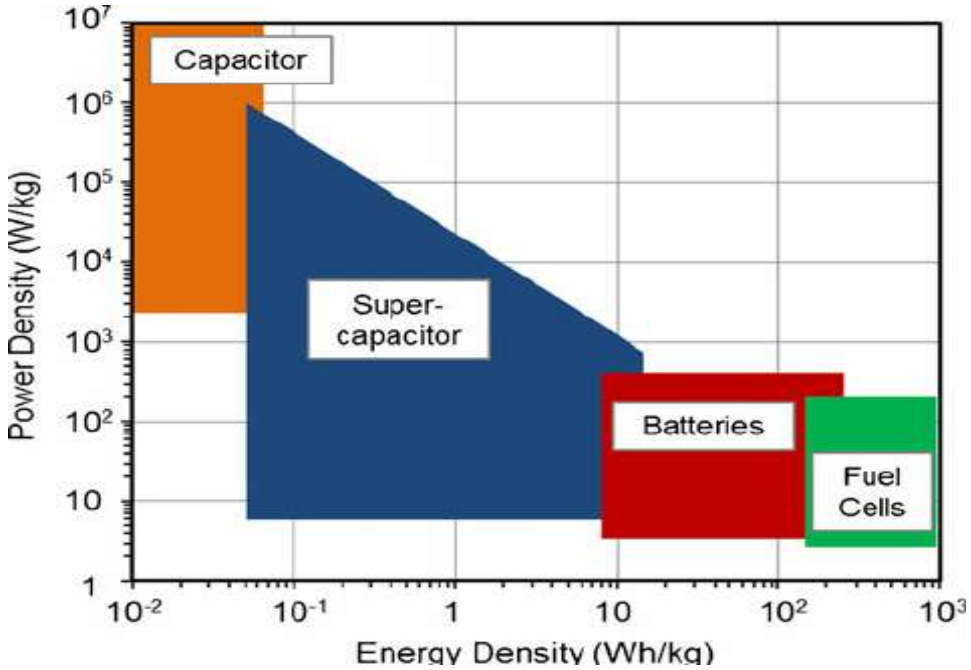

Figure 1: Ragone plot for four energy storage and conversion devices (Meng *et al.*, 2013).

With the rising demands for supercapacitors, researchers have dedicated massive efforts to develop advanced electrode materials with remarkable capacity and superb cycle stability (Mondal *et al.*, 2017). Carbon-based electrode materials have kindled interest as precursor materials for preparation of porous carbons not only because of impressive stability and abundant availability (Yu *et al.*, 2017) but also by the fact that they exhibit superb surface area of approximately 3000 $m^2g^{-1.}$ However, the capacitance is still low for independent devices, ranging from 100 - 300 F g^{-1} (Liu *et al.*, 2015). To raise the capacitance of carbon materials, a typical strategy is to trigger pseudocapacitance by compositing carbon-derived materials with either high redox transition metal oxides (TMOs) or conducting polymer (Du *et al.*, 2013). The focus of this study was, therefore, to improve the capacitance while still preserving the advantages of electrochemical capacitors such as superior cycling stability and excellent power density by synthesizing and testing electrochemical properties of activated carbon derived from Co_3O_4/TiO_2/Ac composite.

1.2 Research problem and justification of study

Due to the high price of supercapacitor electrode materials, the focus has been to use high conductive porous carbon derived from biomass which does not pose threats to food security. However, affordable electrodes synthesized from most biomass-based porous materials suffer from low capacitance and therefore, new materials are necessary to solve the shortcomings of the current materials with respect to energy density, capacitance, and affordability (Kong *et al.*, 2016). Contrary to carbon materials, transition metal oxides have poor electrical conductivity but exhibit high capacitance that complements weaknesses of carbon material when composited. In line with these arguments, this research explored porous carbon derived from fish bladders composited with Co_3O_4/TiO_2 as electrodes for supercapacitors to cater for both power and energy demands of the upcoming hybrid electric vehicles and handy electric power dependent devices such as laptops and handsets.

In total, Lake Victoria has 254 666 tonnes of Nile perch, an equivalent of 24% of the total fish catch (LVFO, 2014) which gives approximately 5857 tonnes as the fish bladder produced annually. This is an amount that can produce porous carbon enough for commercialization of affordable supercapacitors.

1.3 Objectives

1.3.1 General objective

To evaluate fish bladder derived activated porous carbon/cobalt oxide/titanium dioxide composite materials as electrode materials for electrochemical capacitors.

1.3.2 Specific objectives

The primary focus of the prime objective of the study was accomplished by the aid of two specific objectives:

(i) To synthesize and characterize fish bladders derived activated carbon/cobalt oxide/titanium dioxide composite materials.
(ii) To determine the electrochemical performances of the fish bladders derived activated carbon/cobalt oxide/titanium dioxide composite electrode materials.

1.4 Research questions

(i) What are the physicochemical properties of the synthesized fish bladder derived activated porous carbon/cobalt oxide/titanium dioxide composite electrodes?

(ii) What are the electrochemical performances of the fish bladder derived activated porous carbon/cobalt oxide/titanium dioxide composite electrodes?

1.5 Significance of the research

One of the most significant contributions of this work is the knowledge and expertise gained in the use of fish bladder derived porous carbon/cobalt oxide/titania composites for supercapacitor electrodes. Converting fish bladder waste into porous carbon, replacement of expensive and toxic ruthenium oxide with readily available cobalt oxide and titanium dioxide materials not only solves energy problems but environmental and economical issues involved during the process. The total catch of Nile perch in Lake Victoria is 254 666 tonnes, an equivalent of 24% of the total fish catch (LVFO, 2014) which gives approximately 5857 tonnes as the fish bladder produced annually. This is an amount that can produce porous carbon enough for commercialization of affordable supercapacitors. Additionally, this is a source of income for fishing communities in Lake Victoria and other lakes in East Africa where fishing is a key economic activity (Aloo *et al.*, 2017).

CHAPTER TWO

LITERATURE REVIEW

2.1 Introduction

Electrochemical capacitors have gained fame because of their ability to both attain remarkable cycle life and deliver high power supply which can meet the current energy demands for small electric dependent gadgets like mobile phones to medium sized machines such as hybrid vehicles (Xu *et al.*, 2018). However, in comparison to fuels cells and the commonly used lithium-ion cells, supercapacitors display very low energy density (Pham *et al.*, 2018). This, therefore, means that in order for supercapacitor to compete with its counterparts, this problem must be addressed without compromising the existing advantages (Achour *et al.*, 2017). Pursuing higher energy density has become a center of interest of the ongoing research on materials and electrolytes that aims at advancing supercapacitor technology. This advancing technology is expected to make a leap to the next level of energy storage. This, section, therefore discusses the pros and cons of the available electrode materials and electrolytes for supercapacitor, and the possible combinations for application in a supercapacitor.

2.2 Energy storage principle in electrochemical capacitors

The main components of an electrochemical capacitor are two electrodes, separator, and electrolytes (Miao *et al.*, 2015), see Fig. 2. Electrode materials and electrolytes play a pivotal role because of the fact that electrode properties and voltage window of the electrolytes directly determines the energy density of a supercapacitor (He *et al.*, 2016; Sk *et al.*, 2016). The equation below gives a summary of this information

$$E = \frac{1}{2} C \times V^2 \tag{1}$$

where C represents specific capacitance, E stands for energy density and cell voltage has been abbreviated as V (Ma *et al.*, 2017).

Scientifically proven fundamental energy storage principles are electric double layer capacitance (EDLCs) and pseudocapacitance (Gu *et al.*, 2015). Electric double layer capacitors storage mechanism has a fast charge ability, quick power delivery, better power performance and excellent cycle stability due to the fact that it can tolerate millions of cycles, unlike batteries that attain a maximum of a few thousands of cycles (Aradilla *et al.*, 2017). Despite the fact that EDLCs have shown interestingly better cycling stability than batteries but they have low energy density and therefore research on this electrochemical is targeting on improving this low energy performance (Iro *et al.*, 2016).

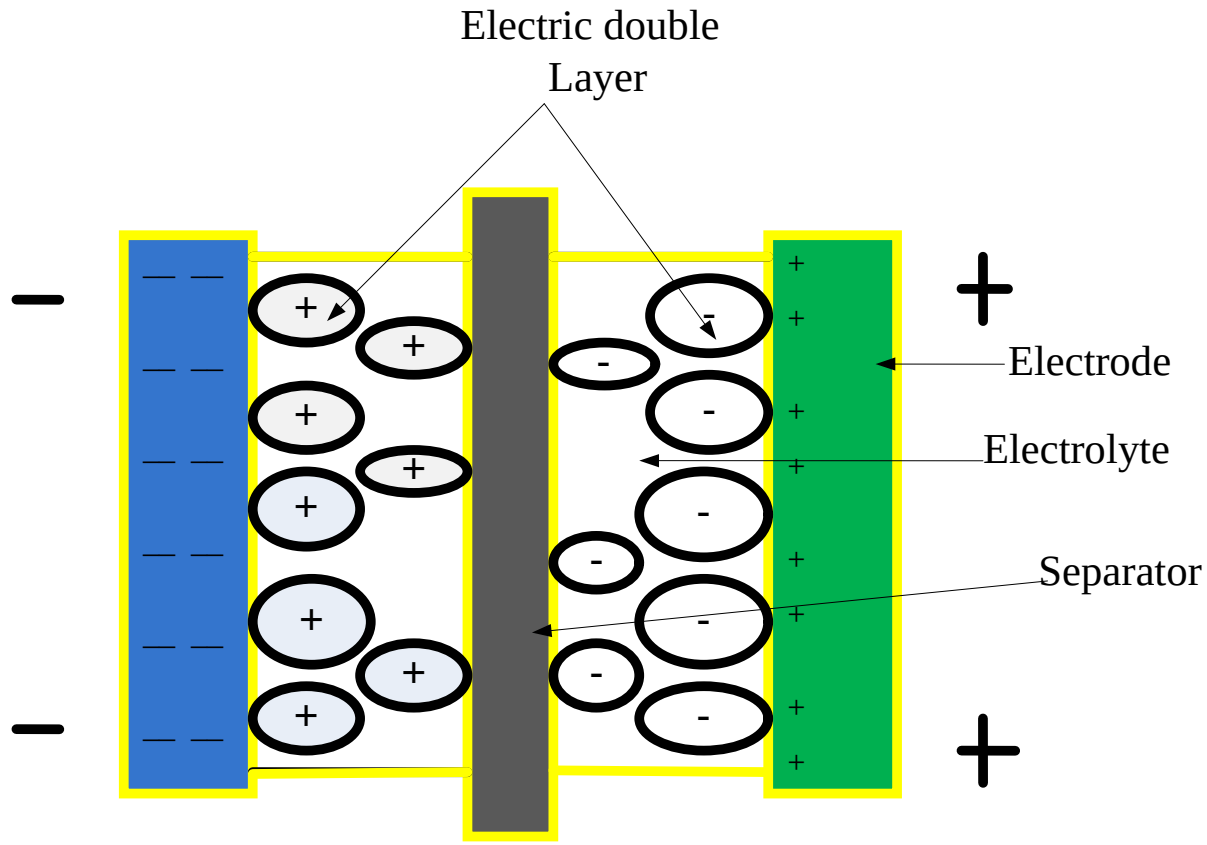

Figure 2: Diagram showing the generation of electric double layer capacitance.

Unlike EDLCs, pseudocapacitance incorporates transition metal oxides/hydroxides, conductive polymers or their composites for fast faradaic reactions in and on the electro-active electrode materials (Junjiao *et al.*, 2015). A pseudocapacitive material undergoes reduction and oxidation when a potential difference is created and this leads to transfer of charges across the double layer, causing a flow of faradic current passing through the electrodes of an electrochemical capacitor. It is from this faradic process involved that comparatively higher energy density is achieved in pseudocapacitors than electrochemical capacitors. Generally, a double layer capacitance is characterized by nearly rectangular voltammogram curve and triangularly shaped time dependent charge-discharge curves whereas pseudocapacitance shows non-rectangular and non-triangular shapes because of the observed reduction and oxidation peaks (Edison *et al.*, 2018a).

2.3 Electrochemical capacitor electrode materials

Physiochemical properties such as morphology, pore size, surface area, specific capacitance, mechanical and structural stability of electrode materials have been reported to determine the overall performance of an electrochemical capacitor including but not limited to power density and energy density (Karnan *et al.*, 2017; Lee *et al.*, 2018). In this regard, extensive research on electrode materials has been done to optimize the aforementioned properties.

For instance, carbon-based materials like activated carbons (Acs) (Hou *et al.*, 2017), carbon fibers (CFs) (Moreno *et al.*, 2017), graphene (Wang *et al.*, 2016) and carbon nanotubes (CNTs) (Guan *et al.*, 2015) have been preferred because they not only provide high surface area and low electrical resistance but their structural stability is also very high. Diversely, oxides and hydroxides of transition metal oxides like cobalt oxide, conducting polymers (polyaniline) and their composites have gained special attention because of their high specific capacitances emanating from their good pseudocapacitive properties (Rose *et al.*, 2018).

2.3.1 Activated carbons

Activated carbon exists in divergent shapes and dimensions like zero-dimension, one-dimension, two dimensions and three-dimension for carbon onions, CNTs, graphene oxide, and carbon-derived carbides respectively. This different dimensions have come along with attractive properties including but not limited to high porosity, reduced electrical conductivity

and remarkable surface chemistries (Cheng *et al.*, 2015). Among these carbon materials, agricultural biomasses derived porous carbon show competitive advantages in supercapacitor practical applications because of their low production costs, availability, good electrical conductivity, large specific surface areas, superb cycling stabilities, and environmental compatibility (Liu *et al.*, 2015). This kind of unique properties of porous carbon has drawn great attention to a number of researchers in recent studies. Just to mention a few, microporous and mesoporous carbon prepared by means of chemical activation (KOH) method at 600 °C for 1 h afforded BET specific surface area of ~800 m^2 g^{-1}. This BET area was among other factors that contributed up to specific capacitance of 390 F g^{-1} at 0.5 A g^{-1} (Karnan *et al.*, 2017). Researchers developed a practical and profitable technique that was used to activate cattail biomass-derived porous carbon via carbon dioxide activation. They also observed a satisfactory specific surface area of 441.12 m^2/g and specific capacitance of 126.5 Fg^{-1} at 0.5 Ag^{-1} between a broad voltage window from -1.0-0 V in 6 M KOH electrolyte (Yu *et al.*, 2017). Lately, it has been reported that bamboo-derived mesoporous activated at 900 °C exhibit a BET area of 2221.1 m^2g^{-1}, ample specific capacitance of 293 F g^{-1} at 0.5 A g^{-1} and excellent rate capability of 193.8 F g^{-1} at 20 Ag^{-1} conducted in 3 M KOH electrolyte (Zhang *et al.*, 2018b).

Despite the fact that biomass-derived carbons have gained scientific attention because of their economic advantages like availability and scientific advantages like good stability and superb surface area, their energy density is still below the mark (Lintong *et al.*, 2016). To improve the performance of these porous carbons for practical application, there is a need to understand the relationship between specific capacitance and surface chemistry which depends on the pores, functional groups present, pore volume, pore size distribution, and interconnectivity (Zou *et al.*, 2018). All these properties have a role to play on the performance of an electrode of a supercapacitive. For example, it should be pointed out that narrow microspores show molecular sieving effect and therefore their contribution to double layer capacitance is very negligible (Raymundo *et al.*, 2006). Activated carbons with pores less than 0.68 nm have been reported to deny access of organic electrolytes with an exception of acetonitrile organic electrolyte electrode, which shows contradictory observation of dramatic increase in specific capacitance as the pore size becomes smaller below 1 nm in size (Chmiola *et al.*, 2006).

Generally, both poor electrical conductivity and low surface area of an electrode material results to low supercapacitor performance but surprisingly, higher surface area can lead to low electric conductivity (Stankovich *et al.*, 2007). Such a phenomenon, therefore, requires that these parameters be optimized so as to maximize the supercapacitive performance of carbon materials (Long *et al.*, 2015). In line with the current problem of low energy density associated with EDLCs, most researchers have opted to explore either the use of naturally hetero-doped carbons or artificially doped carbon to trigger pseudocapacitance (Bing *et al.*, 2016). Artificial doping of carbon materials has been tried by a number of researchers (Paraknowitsch and Thomas, 2013). Unfortunately, this process is expensive, time-consuming and employs toxic precursor for doping such as pyrrole and ammonia, these limitations have compromised its practical applicability (Deng *et al.*, 2015). This, therefore, means that naturally, doped carbon stands out as a better and affordable option to utilize the advantages of heteroatoms in the carbon framework. These advantages include high electronic conductivity, good wettability, and high capacitance from pseudocapacitance (Cai *et al.*, 2017). On this subject, natural pomelo peel derived carbon has been investigated; it afforded substantial amount of nitrogen content (4.47%) and high BET surface area of 1104 m^2g^{-1}. Additionally, this carbon displayed comparatively good capacitance of 208.7 F g^{-1} at 1 A g^{-1} accompanied with an energy density of 7.3 Wh/kg in 1 M H_2SO_4 electrolyte (Fu *et al.*, 2018). Chitosan as a precursor was used to synthesize nitrogen-containing porous carbon by hydrothermal treatment method (250 ℃, 14 h) prior chemical activation using KOH. A descent specific surface area of 2200 m^2 g^{-1}, nitrogen content of 6.3% and most importantly displayed decent specific capacitance of 305 F g^{-1} (Linfeng *et al.*, 2016).

Since graphitic materials exhibit better electrical conductivity, Atchudan and his group used a direct hydrothermal technique to synthesize high nitrogen-containing graphitic carbon sheets derived from unripe peach extracts. This carbon showed moderate specific capacitance of 176 F g^{-1} at 0.1 A g^{-1} with fairly good cycle stability beyond 2000 cycles (Atchudan *et al.*, 2017). Fish bladder as a rich source of proteins carbonized and activated at 550 ℃ had a surface area of 3068 m^2 g^{-1}, the high specific capacitance of 410 F g^{-1} accompanied with good cycle stability of only 14% loss of capacitance over 10 000 cycles (Hu *et al.*, 2016). This study later motivated Han and coworkers to investigate fish gill-derived porous carbon as a naturally doped carbon precursor. They reported a high specific capacitance of 334 F g^{-1} at 2 A g^{-1} in 6 M KOH electrolyte and admirable retention capacity of 93% at 40 A g^{-1} (Han *et al.*, 2017).

2.3.2 Carbon aerogels derived from biomass

This a group of lightweight materials targeted because of their unique properties like high porosity, low mass densities, large surface areas, excellent electrical conductivity, and excellent chemical stabilities deemed necessary for energy storage (Cheng *et al.*, 2016). Recently, carbon aerogels from pyrolysis of biomass sources such as prolifera-green-tide have been investigated and qualified to be potential candidates for supercapacitor applications evidenced from their inspiring properties such as extraordinary recycling performance (Cui *et al.*, 2016). In a different study, recycled carbon aerogels electrode showed high stability and specific capacitance of 194.7 F g^{-1} (Lai *et al.*, 2016). Porous carbon aerogels doped with nitrogen prepared from low-cost mild method exhibits high conductivity, a good capacitance of 291 F g^{-1} and strong ability to retain up to 96.8% of capacitance after 10 000 cycles (Cai *et al.*, 2017). It is reported that aerogels prepared by pyrolysing carbides in the presence of chlorine at 700 °C and 1000 °C and further activating with carbon dioxide provided an average specific capacitance of 170 F g^{-1} in an ionic liquid electrolyte (Oschatz *et al.*, 2017).

Xi and his group synthesized bamboo-derived aerogel with large surface area and attractive ability to flex up to 86% when stressed with a pressure of about 23 KPa. They also observed high specific capacitance of 381 F g^{-1} and 90% of capacitance after 2000 cycles at 200 mV/s (Xi *et al.*, 2017). The above aforementioned capacitance was higher than nano cellulose-derived porous carbon aerogels with a specific capacitances of 302 F g^{-1} and 205 F g^{-1} at a current density of 0.5 A g^{-1} and 20 A g^{-1} respectively with ability to retain 92% of the initial capacity beyond 4000 cycles (Zu *et al.*, 2016). In line with these afore-mentioned observations, researchers reported a simple, environmental compatible synthesis of glucose-derived three-dimensional carbon aerogel after chemical activation with NaOH. They reported not only excellent stability of 1% capacity loss after 1000 cycles but they also reported values of 299 F g^{-1} and 41.52 Wh kg^{-1} as specific capacitance and energy density, respectively (Jing *et al.*, 2017).

2.3.3 Activated carbon/graphene composites

The main limitation of carbon-based electrodes is their low specific capacitance arising from their poor connectivity between large twisty pores despite the fact that they have the

advantage of high specific surface area (To *et al.*, 2015). This drawback has ignited researchers to investigate carbon composites with an intention to advance the performance of porous carbon. Differently, graphene is one of the most influential partners with carbon due to its competitive advantages like high porosity, flexible structure, excellent electrical conductivity and ability to withstand high temperatures (Zhao *et al.*, 2018). In addition to this, three-dimensional (3D) graphene have been reported to shorten the ion transport pathway and to facilitate free electrolytes ion diffusion in electrodes (Zhang *et al.*, 2018a). However, practical application of graphene as supercapacitor electrodes in commercial scale is hampered by the fact that it undergoes irreversible aggregation and restacking (Liu *et al.*, 2017a). Seeking alternative methods such as investigating graphene composites have been investigated. This has lead to a series of research targeting composites of graphene and activated carbon which were expected to come along with a number of advantages including improved surface area, conductivity, and comparatively better pore size.

Although the discovery of graphene was termed a huge scientific leap because of its ground breaking properties, the dispersed problem of graphene is calling for more attention so as to commercialize graphene. Chen and his group activated graphene/carbon with KOH, which affords an improved specific surface area of 798 m^2 g^{-1}. This substantial surface area of the composite might have contributed to the observed specific capacitance of 122 F g^{-1} and energy density of 6.1 Wh/kg (Chen *et al.*, 2012). Activated carbon/graphene composite with micropore volume conducted in aqueous solution afforded higher specific capacitance of 300 F g^{-1} at 0.1 A g^{-1} with adequate cycle stability of 76% at 8 A g^{-1} as compared to graphene without carbon (Fan *et al.*, 2014). Despite the fact that literature has reported great achievements for carbon/graphene composites, further, improvement has been realized by altering the physical properties such as particle size, morphology, and composition of graphene, and carbon composites. Taking advantage of these properties, Xie and co-workers doped a composite of porous carbon and graphene. This composite doped with nitrogen was able to exhibit 381.6 F g^{-1} at 0.1 A g^{-1} (Xie *et al.*, 2016).

2.3.4 Activated carbon/carbon nanotubes composites

In a list of diverse electrode materials used for supercapacitor applications, carbon nanotubes (CNTs) have shown attractive features including but not limited to high porosity, low electrical resistance, low density and admirable electrolyte accessibility (Wan *et al.*, 2017).

The hollow stable structures of Carbon Nanotubes can upgrade the performance of carbon-based materials because they significantly contributes to accessibility, electric conductivity, and transportation of both ions and electrons in the active materials (Yang *et al.*, 2016).

For this reason, Islam and His group argue that the attachment of CNTs on CF can increase ion diffusion, which is a key parameter in realizing excellent electrochemical capacitive properties. They reported that CF exhibited 3.5 times less specific capacitance than the composite (143 F g^{-1} at 1 A g^{-1}). In addition to the aforementioned advantages, CNT–CF exhibits good flexibility and therefore has the ability to address the rising demand for flexible energy storage devices (Islam *et al.*, 2016). With quite a number of strategies laid down to commercialize carbon, carbon doping is in the spotlight because of the ability to donate electrons thus improves the distribution of charges around atoms of carbon resulting into an improved number of active sites for redox reactions. Focusing on nitrogen-containing functional groups, electrical conductive CNTs and Zeolitic imidazolate framework (ZIF-8) carbon doped with nitrogen was investigated. Electrodes fabricated from this composite exhibited not only high BET surface area of 287 m^2 g^{-1} and specific capacitance of 324 F g^{-1} but also delivered superlative capacity retention of 93.5% after 1000 cycles (Wan *et al.*, 2017).

Carbon nanotube deposited on conducting polymers showed better pseudocapacitance effects for carbon nanotube/polymer with the highest specific capacitance of 87 F g^{-1} and higher energy density of 1.82 W h kg^{-1} than CNT/carbon composites which afforded 21 F g^{-1} and 0.58 W h kg^{-1} capacitance and energy density, respectively (Xiao and Zhou, 2013). Graphitic CNT electrodes have raised the eyebrows of a number scholars because of their outstanding abilities, they have low electrical resistance, good mechanical stability, thermal stability and high surface area because of their tube-like morphology (Wang and Kaskel, 2012).

One of the main drawbacks of porous carbon doped with nitrogen is low volumetric capacitance because carbon is a low density material (Tao *et al.*, 2013). This challenge has been addressed by several scholars by optimizing on the advantages of individual materials. For instance, in a study conducted by Jiao and his group, hollow activated carbon fiber - CNT have been reported to exhibit promising supercapacitive features making a pronounced contribution towards the attained specific surface area of 825 m^2 g^{-1} and maximum specific capacitance of 240 F g^{-1} in 1 M H_2SO_4 solution (Jiao *et al.*, 2018).

2.3.5 Conductive polymers/activated carbon

These are long chains of polymers basically organic in nature with an electric conducting ability arising from their conjugated bond system. Good conductivity and flexibility are one of the main properties that give polymers an edge over other electrode materials especially with the escalating need for flexible supercapacitors (Shown *et al.*, 2015). In comparison to TMOs, conductive polymers show advantages like simple doping, low cost, and most importantly they can be used to fabricate wearable and flexible devices (Ansari *et al.*, 2017). Unfortunately, practical application of conductive polymers like polyaniline (PANI) in the field of energy is prone to structure deformation leading to capacitance fading within few charge/discharge cycles (Asen *et al.*, 2018). Taking advantage of excellent cycle stability of activated carbons, scientists have composited polymers with carbon to improve the cycle stability of polymers and improve doping-dedoping chemistry ability of carbon as a mutual benefit.

For instance, activated carbon from coconut shell composited with PANI was synthesized by oxidizing a monomer with potassium persulphate in presence of tetraflouroboric acidic displaying capacitance of 99.6 F g^{-1} at 0.5 mA g^{-1} and 77 F g^{-1} at 2 mV s^{-1} (Vighnesha *et al.*, 2017). A composite of polyaniline and activated carbon derived from rice husk (60 wt% polyaniline) also shows good electrochemical properties displaying top most capacitance of 465 F g^{-1} in 1 M H_2SO_4 at 0.2 A g^{-1} (Lebedeva *et al.*, 2018). With a clear interest in the flexibility of carbon aerogels and availability of biomass-derived carbon, Yu and his group fabricated binder-less electrodes from a composite of carbon aerogel and polypyrrole. They reported high areal capacitance of 419 mF cm^{-2} at 1 mA cm^{-1} (voltage range of 0.0–0.8 V) in a 1 M H_2SO_4 electrolyte. Additionally, the electrodes demonstrate good capability by capacitance fading down to 86.4% after 3000 cycles (Yu *et al.*, 2018).

2.3.6 Transition metal oxides and their composites

An ideal transition metal oxide for energy storage applications should have low electrical resistance, have multiple oxidation numbers in the same phase with free ions that can intercalate into TMOs lattice for fast redox reactions, high surface area and should also be electrochemically active (Yadav *et al.*, 2018). In a couple of years, we have experienced progressive research on different TMOs like Co_3O_4, Fe_3O_4, NiO, TiO_2, MnO_2, and RuO_2 as

potential pseudocapacitor materials for electrode so as to take advantage of their high theoretical specific capacitance (Zhao *et al.*, 2016). Ruthenium oxide has shown its prowess than other TMOs by delivering outstanding performance evidenced by the high capacitance of approximately 1300 F g^{-1}, wide operational potential window, long cycle life, low electrical resistance, decent rate capability and excellent electrochemical reversibility (Tajik *et al.*, 2017). Taking advantage of these properties, RuO_2 nanosheets were synthesized prior to electrode fabrication which later revealed an ideal capacitive behavior. When scanned at 5 mV s^{-1}, the specific capacitance of 600 F g^{-1} was observed in 3 M KCl aqueous electrolyte (Vijayabala *et al.*, 2017). This excellent pseudocapacitive behavior of RuO_2 reported in the literature inspired scientists to deeply investigate this transition metal oxide. For instance, researchers used the hydrothermal method to uniformly deposit hydrous RuO_2 nanoparticles onto nitrogen-doped mesoporous carbons and impressively observed outstanding specific capacitance of 1733 F g^{-1} (Zhang *et al.*, 2014a). Despite the above aforementioned advantageous, high cost, scarcity, and toxicity are the main hurdles that hinder practical application and possible commercialization of RuO_2 (He and Li, 2018). This has, therefore, propelled an idea of finding profitable and environmentally compatible electrode materials like NiO, Co_3O_4, MnO_2, and TiO_2 as alternatives to RuO_2 (Xie *et al.*, 2013).

Though with high electrical resistance (10^{-5} –10^{-6} S cm^{-1}) (Wang *et al.*, 2017a), manganese oxide has the highest oxidative state (VII) in the whole periodic table and high theoretical capacitance (1370 F g^{-1}) (Yating *et al.*, 2018). Manganese oxide has also been reported to be the second widely investigated electrode material after RuO_2 because of its availability and compatibility with the environment (Anilkumar *et al.*, 2017). Interestingly, when aqueous solutions are used as electrolytes for manganese oxide electrodes, manganese oxide electrodes show ideal capacitive response and high-rate capability because of wide potential window, making them better candidate than cobalt oxides and nickel oxides that are mostly used in strong alkaline electrolytes (Chen *et al.*, 2017).

Inspired by these unique properties, Gnana and his group used chemical precipitation method to synthesize manganese oxide Mn_3O_4. They exhibited high specific capacitance of 322 F g^{-1} at a lower current density of 0.5 mA cm^{-2} and capacity retention of 77% after 1000 cycles in 1 M Na_2SO_4 (Gnana *et al.*, 2015). This kind of performance was slightly higher than Mn_3O_4 nanorods prepared through precipitation with specific a capacitance of 298 F g^{-1} with a strong

ability to retain up 95.1 % of the primary capacitance after 1000 charge discharging cycles (Aghazadeh *et al.*, 2016). Motivated by the ballooning market for portable rollable electronics, implantable chips, flexible sensors and wearable electronics (Wang *et al.*, 2016), Wu and his group fabricated a flexible 3D electrode. They not only reported decent specific capacitance of 298 F g^{-1} at 0.5 A g^{-1} but observed cycling stability of 90.3% retention capacity beyond 5000 cycles in 1 M Na_2SO_4 (Wu *et al.*, 2018).

Nickel oxide has recently been on demand as a storage material suitable for supercapacitor electrodes. It enjoys significant attention because of its availability, chemical stability accompanies with an amazing theoretical specific capacitance of approximately 2573 F g^{-1}, (Simon *et al.*, 2018). Vidhyadharan and his group evaluated one of the best electrodes from nickel oxide nanowires. Interestingly they observed satisfactory specific capacitance of 670 F g^{-1} with no capacitance loss even after 1000 cycles and coulombic efficiency of 98% chemical precipitation method (Vidhyadharan *et al.*, 2014).

It is crucial to mention that different shapes and morphologies of NiO such as nanoflowers and nanosheets show different electrochemical performances simply because of the difference in utilization of electrochemical properties of the working electrode (An *et al.*, 2016). For instance, different sizes of NiO nanoparticles display different specific capacitance like 6 nm size particles deliver capacitance of 449 F g^{-1}, 323 F g^{-1} for particles with approximately 21 nm and 63 F g^{-1} for particles with approximately 41 nm all scanned at 5 mVs^{-1} (Duraisamy *et al.*, 2016). However, due to high electrical resistance and less utilization of active material sites, NiO electrode has displayed low specific capacitance in supercapacitor applications. To unravel this issue of low conductivity, NiO has been composited with conducting carbon materials (Simon *et al.*, 2018). This strategy has be argued that it increases the total number of active sites and consequently improves the transportation of both electron and ion in the material (Chen *et al.*, 2018).

In line with the aforementioned advantages of carbon materials, NiO/RGO electrodes were investigated. They exhibited a promising specific capacitance of 590 F g^{-1} at 1 A g^{-1}, high rate capability of 88% retention at a high rate of 15 A g^{-1} and interestingly recorded no loss in specific capacitance after 1000 cycles (Kahimbi *et al.*, 2017). In a dissimilar study, challenges associated with single metal oxides were addressed by synthesizing nickel-manganese oxide composite material. This composite successfully delivered specific

capacitance of 407 F g^{-1} at 1 A g^{-1} and superior retention capacity of up to 98.4% after 1000 cycles in KOH electrolyte (Wei *et al.*, 2017).

On top of this supremacy in terms high stability and low cost, titanium dioxide presents yet another interestingly divergent advantage of biocompatibility which makes it find practical application in the emerging supercapacitor implantable and wearable devices such as pacemakers, implanted chips and power bodysuits (Zhou *et al.*, 2015). Although TiO_2 nanomaterials had been given less attention because of poor conductivity a number of scientists share the view that it can improve cycle stability of other active materials because of its low volume expansion/contraction during electrochemical cycling hence improving the cycle life of supercapacitors (Baraia *et al.*, 2017). Driven by this fascinating property, Pham and his group used simple sol-gel method to synthesize a composite of hydrogenated TiO_2 and reduced graphene oxide (RGO) nanosheets. Surprisingly, they reported low capacitance of 51 F g^{-1} at 1.0 A g^{-1} with a competitive capacity dropping down to 80% after 10 000 cycles (Pham *et al.*, 2018). Additionally, carbon has been on the front line in improving the electrical conductivity of TMOs, its combination with TMOs such as TiO_2 has come with a plus as it also improves the concentration of ions on carbon surface. This phenomenon, therefore, improves wettability and significantly contributes towards improved specific capacitance of EDLCs (Seo and Park, 2010). Recently, a composite of TiO_2 nanotubes and graphene nanosheets was synthesized for both supercapacitors and absorbents applications. It disclosed a specific capacitance of 338 F g^{-1} at a scan rate of 5 mV s^{-1} and lifelong stability by maintaining about 93.3% specific capacitance after 3000 cycles in 1 M Na_2SO_4 electrolyte (Zhang *et al.*, 2017b). To keep pace with the ever-rising demand for wearable electronics, Xu and his co-workers synthesized flexible composite of polypyrrole (PPy) and TiO_2. They garnered better capacitance of 733 F g^{-1} at 0.6 A cm^{-1} as compared to single TiO_2 (366 F g^{-1}) (Xu *et al.*, 2017).

Cobalt oxide is with no doubt one of most fascinating material with superb theoretical capacitance and relatively low environmental footprint. Unfortunately, it experiences large volume expansion and contraction which to poor cycle stability reported in previous work (Numan *et al.*, 2016). One of the most efficient methods to unravel the unsatisfactory cycling stability is to integrate Co_3O_4 nanoparticles with carbon materials (Li *et al.*, 2018a). In this regard, Hout and his group successfully introduced a highly conductive RGO to Co_3O_4 to

achieve to reduce electrical resistance hence improving the swift movement of ions in the composite. The composite (Co_3O_4/RGO) delivered a capacitance of 531 F g^{-1} at a 0.1 A g^{-1} with capacity retention ability of 64% after 2000 cycles (Hout *et al.*, 2017). To further maximize the electrochemical potential of Co_3O_4, a number of research groups have come up with different strategies such as synthesis of Co_3O_4 with different morphology and different design in pore sizes.

It has been argued that rationally controlled structure may accelerate ion diffusion and improve the mechanical properties of Co_3O_4 (Li *et al.*, 2018b). This has been an inspirational fact for scholars to investigate the effect of different morphologies. For instance, Co_3O_4 nanorod electrodes synthesized and evaluated in the presence of 6 M KOH electrolyte at a scan rate of 10 mV s^{-1} delivered high specific capacitance of 226.3 F g^{-1} with excellent stability of 76% capacity retention after 500 cycles (Jang *et al.*, 2017). In a different study, slanting angle synthesis method was applied to grow Co_3O_4 nanorod film. In spite that the capacity retention was as low as 62% after 2000 cycles but a promising specific capacitance of 2875 F g^{-1} was reported as a function of an impressive energy and power of 57.7 Wh Kg^{-1} and 9.5 kW kg^{-1}, respectively (Kannan *et al.*, 2018).

2.3.7 Ternary metal oxides

In the pursuit for higher specific capacitance, researchers have combined TMOs as materials for supercapacitor applications. This idea has been propelled by the fact that ternary metal oxides have a better supercapacitive performance than a single TMOs because of synergistic effects (Wu *et al.*, 2012). Ternary metal oxides combine three different electrode materials to form one electrode; this exhibits comparatively higher electrochemical performance than single TMOs because of their ability to exist in different oxidation numbers (Chen *et al.*, 2015). Provoked by this idea, iron manganese oxide (Fe-Mn-O) was synthesized by Zhu and his group. Unfortunately, this combination showed low specific capacitance of 86.7 F g^{-1} at 1 A g^{-1} when investigated between a voltage window of 0.2 to 1.0 V (Zhu *et al.*, 2016). On the other hand, Yong and Xiao took advantage of stable TiO_2 nanotube and superior RuO_2 to synthesize a composite of RuO_2/TiO_2 nanotubes by using different ratios of RuO_2: TiO_2 nanotubes. They reported excellent specific capacitance of 1263 F g^{-1} using gel polymer PVA–H_3PO_4–H_2O electrolyte (Yong and Xiao, 2004).

In fact, a combination of only TMOs has not met the expected mark, most of the reported specific capacitance is below that of RuO_2, and therefore researchers have found it necessary to combine these double transition metal hydroxides/oxides with electric conductive materials like carbon (Fang *et al.*, 2018). Basing on this scientific statement, Lei and the group observed remarkable capacitance of 2050.6 F g^{-1} at 1 A g^{-1} and capacitance retention of 84% after 1000 cycles from a composite of graphene and nickel-cobalt double hydroxide. This remarkable capacitance may have been contributed by the high electric conductive graphene in the composite (Lei *et al.*, 2018).

Other strategies to improve electrochemical performance is by using binder less electrode materials, this binder less electrode reduce both electrical resistance and the facile process of electrodes (Kim *et al.*, 2018). As binder less electrode, Co_3O_4@$NiCo_2O_4$/N-doped graphene exhibits remarkable capacitance of 2430 F g^{-1} at 1 A g^{-1} and 93.7 % capacitance retention after 5000 cycles (Ying *et al.*, 2018). In a different study controlled hydrolysis process was used to a composite nickel oxide, cobalt oxide and single wall carbon nanotube ($NiCo_2O_4$−SWCNT). Both amazing specific capacitance of 1642 F g^{-1} and cycling stability of 94.1% retention capacity after 2000 cycles were observed from this composite (Wang *et al.*, 2012). Most recently, it has been reported that CC/NiO/MnO_2 supercapacitor electrodes exhibit increased supercapacitive performance of both areal capacitance and gravimetric capacitance of 316.37 mF cm^{-2} and 204.3 F g^{-1}, respectively at 50 mV s^{-1}. Additionally, excellent cycling stability of 89% after 2200 cycles was also reported from this composite (Xi *et al.*, 2017).

A novel hybrid electrochemical capacitor fabricated by simply coating finely thin MnO_2 film to Zn_2SnO_4 composited with flexible carbon microfibers (CMFs) affords capacitances of 621.6 F g^{-1} and 642.4 F g^{-1} at 2 mV s^{-1} and 1 A g^{-1} respectively in 1 M Na_2SO_4 electrolyte. This composite (MnO_2/ Zn_2SnO_4/CMF) displayed satisfactory abilities such as high specific energy and high specific power of 36.8 Wh kg^{-1} and 32 kW kg^{-1} at 40 A g^{-1} respectively with superior stability evidenced by the ability to dispatch 98.8% of the initial capacity after 1000 cycles (Bao *et al.*, 2011). Wang and his group investigated $NiCo_2O_4$–RGO composite and observed capacitance of 835 F g^{-1} at 1 A g^{-1} and 615 F g^{-1} at 20 A g^{-1}. One of the most fascinating properties of the electrodes was the ability to display a considerable increase in capacitance with an increase in cycling numbers up to 1050 F g^{-1} even after at 450 cycles and

ability to maintain a constant value of 908 F g^{-1} (better capacitance than the initial value) after 4000 cycles (Wang *et al.*, 2011). Iron manganese oxide composites ($FeMoO_4$) doped with graphene demonstrated an improved specific capacitance of 135 F g^{-1} at 1.0 A g^{-1} in comparison with graphene (66 F g^{-1}) or $FeMoO_4$ (96 F g^{-1}) in 1.0 M Na_2SO_3 electrolyte. Comparatively, a composite of graphene with $FeMoO_4$ displayed improved electrical conductivity and better cycle life than pure $FeMoO_4$, signifying the importance of the synergy between the material (Wang *et al.*, 2014).

Titanium dioxide and cobalt oxide composited with carbon material have been reported to show good supercapacitive properties. For instance, Co-doped TiO_2NT delivered specific capacitance of 34.8 F g^{-1} at a scan rate of 5.0 mV s^{-1} (Xiao *et al.*, 2016). A closely related hybrid composite of cobalt oxide coated with titanium dioxide (TiO_2@C/Co_3O_4) was also designed to fabricate asymmetrical electrochemical capacitors. This interestingly displayed significantly higher capacitance of 392.4 F g^{-1} and energy density of 18.54 Wh kg^{-1} at the same scan rate of 5.0 mV s^{-1} (Kim *et al.*, 2016).

2.4 Electrolytes

Just like electrode materials, the contribution of electrolytes cannot be ignored because they have a significant contribution in supercapacitors performance in terms of determining both the electrical conductivity, and breakdown voltage value (Zhang *et al.*, 2014b). Basically, the potential window is proportional to power and energy and therefore determines both power and energy densities of a device (Wanga *et al.*, 2017). An ideal electrolyte should, therefore, have a broad voltage window, low resistance, excellent electrochemical stability, and small solvated ionic radius, high ionic concentration, and high purity, low viscosity, low cost, safe and readily available. Examples of electrolytes widely studied are aqueous, organic electrolytes and ionic electrolytes (Fic *et al.*, 2018). Basically, the higher the concentration of an electrolyte, the better the electrical conductivity and the higher the power output (Liu *et al.*, 2017b).

2.4.1 Aqueous electrolytes

This is a class of electrolytes commonly used because they are ionically conductive, environmentally stable, non-corrosive and environmentally friendly as compared to organic

electrolytes, which are expensive, flammable, toxic and less conductive (Kumar *et al.*, 2015; Zhao and Zheng, 2015). However, potential window of an electrolyte determines the voltage window of a supercapacitor and since the potential window of water is 1.23 V, water-based electrolytes work with a relatively narrow potential window of mostly less than 1.0 V (Rakhi and Lekshmi, 2017). Aqueous electrolytes have been used in many supercapacitors, for instance, cobalt oxide/carbon nanotubes (Co_3O_4/CNTs) nanocomposites successfully synthesized using hydrothermal method exhibited good electrochemical properties such as high specific capacitance of 705 F g^{-1} at 3 A g^{-1} when 1 M KOH was used as an electrolyte (Kumar *et al.*, 2015).

2.4.2 Organic electrolytes

Contrary to aqueous electrolytes which operate in narrow potential window, most organic electrolytes have the ability to operate in a wider voltage window of up to 4 V but the low electrical resistance value prevents them from attaining supercapacitors with high power density (Salunkhe *et al.*, 2015). Organic electrolytes enjoy this fascinating advantage of a wide potential window as this addresses the energy density of supercapacitors. Apart from few organic salts such as tetraethylam- moniumtetrafluoroborate and tetraethyl phosphoniumtetrafluo- roborate, acetonitrile (AN). Propylene carbonate (PC) has also been used as most familiar organic electrolytes for ECs. Recently propylene carbon organic electrolyte and vanadium oxide (VO_2) electrodes were subjected to electrochemical testing in a three electrode arrangement. Symmetrical capacitors from this combination displayed energy and power densities of 46 Wh kg^{-1} and 1.4 kW kg^{-1}, respectively at a current density of 1 Ag^{-1} (Rakhi *et al.*, 2016). Fluorine has recently proved to be a suitable partner with organic electrolyte because of its ability to provide high polarity and wettability for organic electrolytes. Taking advantage of these unique abilities, fluorine-doped carbon electrodes were evaluated and reported to deliver specific capacitance of 168 F g^{-1} accompanied with strong capability to retain capacitance after 10 000 cycles in a mixture of propylene carbonate and tetraethylammonium tetrafluoroborate organic electrolytes (Zhou *et al.*, 2016).

2.4.3 Ionic electrolytes

These are liquid solvent-free electrolytes at room temperature which are basically salts which exist in a molten state at temperatures below room temperature (Salanne, 2017). Ionic liquids

consist entirely of ions which makes them fascinating for different applications. They find applications as new solvents for chemical reactions, in the environment for specific catalysis, storage devices, electrochemical sensing, and electrolytes for energy storage devices (Kasprzak *et al.*, 2018). They have specifically gained fame in supercapacitor applications because of their advantages such as wide electrochemical stability, low flammability, ability to withstand high temperatures and besides they are chemically stable (Osti *et al.*, 2018). Unfortunately, ionic liquids are expensive, have comparatively high internal and ionic resistance than aqueous electrolytes and this, therefore, remains to be an obstacle in the path towards commercialization (Thangavela *et al.*, 2018).

When supercapacitive properties of reduced graphene oxide were investigated in both 1-butyl-3-methylimidazolium hexafluorophosphate (BMIPF6) and sulphuric acid (H_2SO_4), they showed extreme capacitance values of 348 and 158 F g^{-1} in 1 M H_2SO_4 and $BMIPF_6$, respectively (Chen *et al.*, 2011). The ionothermal method was used to synthesize graphene and porous carbon. Specific capacitance of 212 F g^{-1} at 0.5 A g^{-1} in 1-butyl-3-methylimidazolium dihydric phosphate ([BMIm] $[H_2PO_4]$) electrolytes was reported. When a current density of 2 A g^{-1} was used, the electrode showed only 5.8% capacity loss after 10 000 cycles (Hao *et al.*, 2017).

2.5 Synthesis methods

Ongoing advances in energy research with a purpose to commercialize have established a variety of methods to synthesize electrode materials from crystalline to amorphous materials. Commercialization of energy storage devices depends on several factors such as cost, toxicity, availability, and sustainability. This section, therefore, sheds light on different synthesis methods with a special interest on sol-gel method. Different scholars have used different methods like chemical spray pyrolysis (Deokate *et al.*, 2017), co-precipitation method (Karthikeyan *et al.*, 2009), cathodic electrodeposition method (Edison *et al.*, 2018b), and chemical vapour deposition (Wang *et al.*, 2017b), solvothermal method (Lei *et al.*, 2014), hydrothermal method (Wei *et al.*, 2017), sonochemical method (Karthik *et al.*, 2017), sol-gel method (Zhua *et al.*, 2016), Grafting oxidation method (Faraji *et al.*, 2016). However, most of the aforementioned preparation methods have shown limitations as they are tedious, expensive/complicated handling, time-consuming and use toxic chemicals, thus a facile and mild method for electrode materials preparation with excellent electrochemical performance

is highly desired. Among them, the sol-gel process is simple, cheap, results to homogeneous multi-component metal oxide materials and highly scalable (Lin, 1998). Given the above considerations, the sol-gel method was considered in this study for the synthesis of all the composites.

CHAPTER THREE

MATERIALS AND METHODS

3.1 Materials and reagents

The fish bladder was obtained from Lake Victoria Mwanza, Tanzania. The chemicals used were purchased from Sigma Aldrich, they included ammonia solution, titanium isopropoxide, cobalt chloride hexahydrate, sodium hydroxide, potassium hydroxide, and hydrochloric acid whereas carbon black, nickel foam and polyvinylidene difluoride (PVDF) were supplied by MTI Corporation and distilled water was purchased from Arusha Technical College, Tanzania. All chemicals were used without further modification.

3.2 Synthesis of fish bladder-based activated carbon

Fish bladders were washed with distilled water, sun-dried for 5 h, oven dried for 24 h, crushed and carbonized in a horizontal tube furnace (CTF 12/65/550) at 650 °C for 2 h at a ramp rate of 10 ℃ min^{-1} in a nitrogen flow. The obtained carbon chars were initially ground, sieved through a 150 µm sieve and chemically activated at 550 ℃ in the ratio of 3:1 (KOH: carbon) ratio in the presence of nitrogen for 2 h at the same ramp rate in the same tube furnace used for carbonization. Prior washing activated carbon with 1 M HCl solution to consume residual KOH, it was initially cooled down to room temperature. This was later followed by thorough washing with distilled water to remove both KCl and excess HCl in the solution until pH 7 and finally dried at 120 °C for 12 h (Xia *et al.*, 2018).

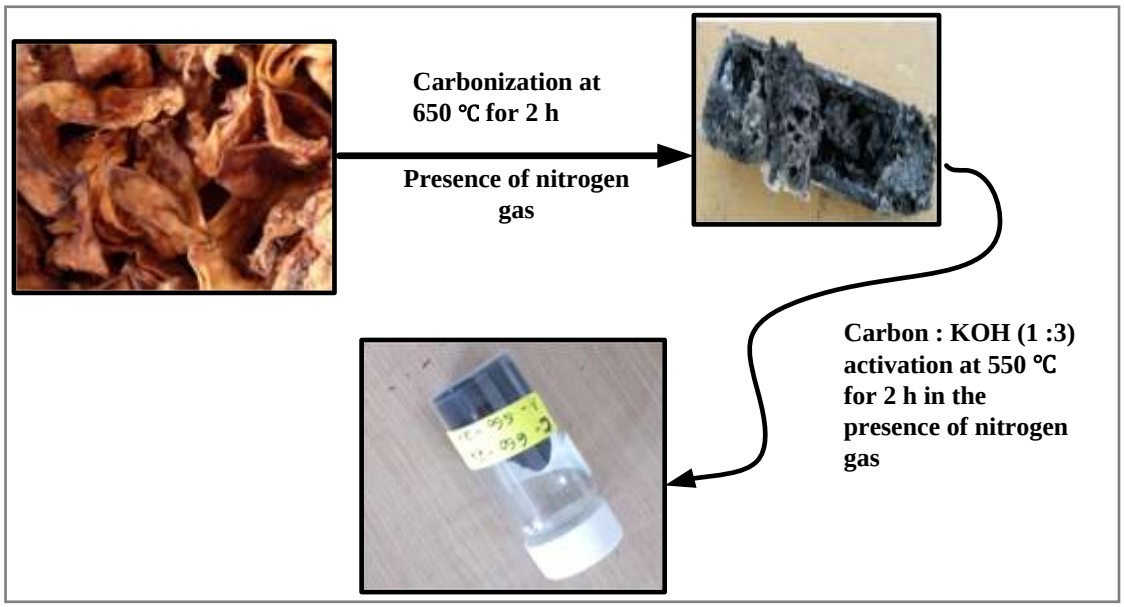

Figure 3: Schematic illustration of the synthesis process of fish bladder-derived porous carbon.

3.3 Preparation of Co_3O_4/TiO_2/Ac, Co_3O_4/Ac, and TiO_2/Ac composites

The composite was prepared by sol-gel synthesis. Approximately 1.367 g fish bladder derived activated carbon was dispersed in 50 mL distilled water followed by 1 g of $CoCl_2.6H_2O$ dissolved in 50 mL of water prior to the addition of 1 mL of titanium isopropoxide ($C_{12}H_{28}O_4Ti$, 97 %) mixed with 50 mL absolute ethanol and then stirred for 20 min. The pH of the solution was regulated to 7 by adding drops of 2 mL ammonia solution resulting into a dark-green mixture which was stirred for 12 h at room temperature and left to settle for 4 h (Jo *et al.*, 2017). The product was filtered and washed with distilled water and ethanol, oven dried for 8 h at 90 ℃ and finally annealed in a box furnace (Lindberg Blue M Model BF51731 BC-1 Thermo Scientific) at 300 ℃ for 2.5 h and the sample was labeled K_2. For comparison, a similar procedure was used to prepare Co_3O_4/Ac without adding $C_{12}H_{28}O_4Ti$, 97 % and the product labeled C_1 while TiO_2/Ac was also prepared using the same procedure without adding $CoCl_2.6H_2O$ and the product was labeled T_1.

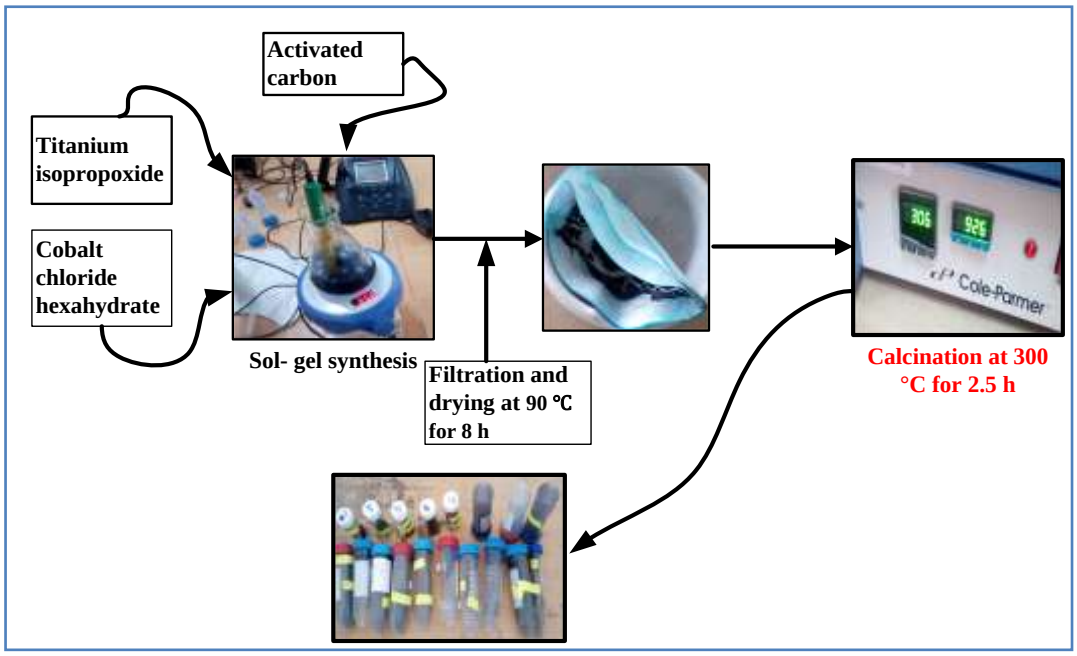

Figure 4: Schematic diagram for the synthesis of cobalt oxide/ titanium dioxide/activated carbon composites.

3.4 Materials characterization

The microstructure characteristics of composite and porous carbon were deeply examined by Field emission scanning electron microscopy (FE-SEM): JSM-7600F Thermo NORAN System 7 coupled with EDS (Japan) under the acceleration voltage of 15 kV. Crystal structures of the synthesized materials were examined by powder X-ray diffraction with Cu kα radiation (λ=0.15406 nm) in 2θ range of 10°-70°. Textural properties of the composite were analyzed by nitrogen adsorption-desorption isotherms at 77.3 K liquid nitrogen by Tristar II 3020 version 2.00 serial no. 1162 instrument. Specific surface area (S_{BET}) was obtained from the BET machine while Barrett–Joyner–Halenda (BJH) method afforded us with the information of pore-size distribution. Determination of functional groups in the composite was investigated by FT-IR (4000- 600 cm^{-1}) using Tensor 27 spectrometer.

3.5 Fabrication of working electrode

To meet demands for practical application of a supercapacitor, it is vital to develop standard electrodes with high active mass loading of approximately 10 mg cm^{-2} (Crosnier *et al.*, 2018). However, this increase in mass loading leads to an increase in resistance and limits access of

electrolyte to the bulk of active materials. As a result, specific capacitance and retention capacity significantly decrease with increase in mass loading of the electrode.

In this study, working electrodes fabrication involved mixing of the active material, conducting carbon (improves the electrode electrical conductivity), polyvinylidene difluoride (PVDF) binder dissolved in N-methyl pyrolidene in the mass ratio of 8:1:1 forming slurry. Nickel-foam (current collector) substrate was soaked in 1 M HCl for 20 min to remove the NiO layer, and then rinsed with distilled water followed by absolute ethanol, and later dried in an oven. The slurry was loaded and pressed on clean nickel foam of size 1 cm^2 with approximate mass loading of 5 mg of the active material. The loaded-nickel foam was finally dried at 60 ℃ in the oven for 4 h.

3.6 Electrochemical tests

Electrochemical tests were analyzed in a three-electrode system with saturated $Ag/AgCl_2$ (KCl) as a reference electrode, platinum was used as a counter electrode whereas a working electrode was prepared as mentioned above. The counter electrode was used to control the current entering the working electrode while the reference electrode maintained at constant potential throughout the experiment. Figure 5 shows the experimental set up used during electrochemical testing.

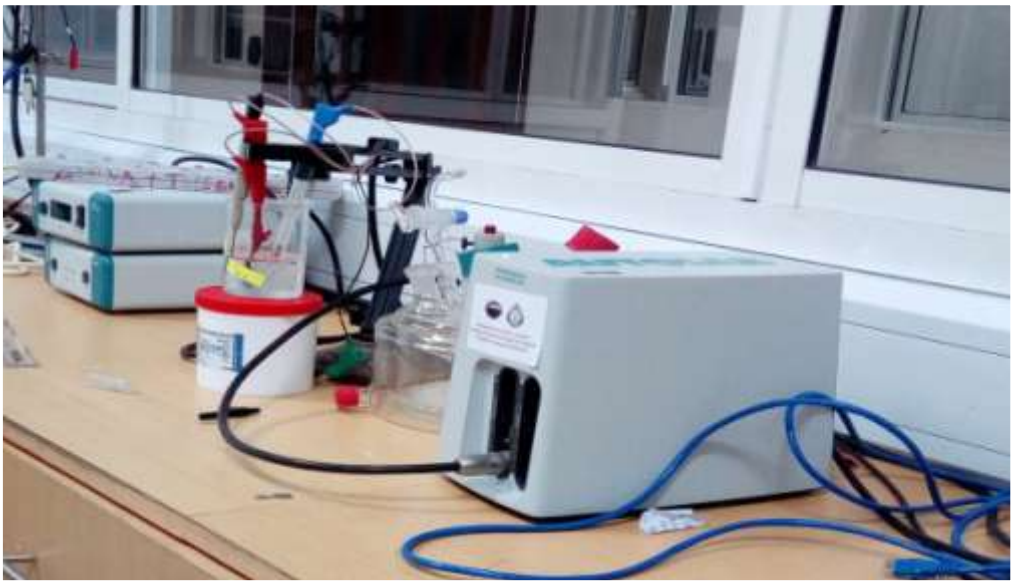

Figure 5: Three-electrode configuration set up for electrochemical testing.

Cyclic voltammetry (CV) is a crucial technique in electrochemical analysis. It is used to determine the voltage range of the device or the electrodes and to perform a kinetic analysis of the device at different scans. In this study, cyclic voltammetry (CV) test was performed on AUTOLAB Potentiostat/Galvanostat (PGSTAT204, AUT50663 Metrohm) in 6 M KOH aqueous electrolyte solution between 0 and 0.5 V versus reference electrode at different scanning rate. Electrochemical impedance spectroscopy (EIS) analysis was carried out by applying an AC voltage with 5 mV amplitude in a frequency range between 0.01 Hz to 100 kHz using FRA32 module attached to PGSTAT 204 in an open circuit.

Specific capacitances (Cs) was calculated from CV using the following equation (Nwanya *et al.*, 2017).

$$Cs = \frac{1}{2mv(\Delta V)} \int_{V1}^{V2} i(V)\,dV \tag{2}$$

where $\int_{V1}^{V2} i(V)dV$ is the absolute integral area of both positive and negative sweep in cyclic voltammogram,v represents scan rate in mV s^{-1}, m denotes the mass of the active material on the electrode in grams and factor 2 represents both positive and negative scans involved. The equation below was employed to calculate the specific capacitance of the active material in the EIS measurements (Enock *et al.*, 2017).

$$C = \frac{-1}{(2\pi f Z'' m)} \tag{3}$$

Where m stands for the mass of active material, f represent the lowest frequency while the imaginary impedance is denoted by Z''.

CHAPTER FOUR

RESULTS AND DISCUSSION

4.1 Introduction

This section introduces and explores different characterization and electrochemical measurements of electrode material. It describes the influence of different physical and chemical properties on electrochemical properties of cobalt oxide/titanium dioxide /activated carbon, cobalt oxide/activated carbon, titanium dioxide/activated carbon and activated carbon. In this chapter, several parameters were tested to assess the practical applicability of the electrode materials such as cycle stability, specific capacitance, electrical conductivity and power delivery of the material.

4.2 X-ray diffraction measurements

As one of the crucial analytical technique, The XRD was employed to determination the phase, crystallinity, and purity of the samples prepared under various conditions. The X-ray beam is applied to the sample experiment with wavelength, λ at different 2θ angles on the sample. Its working principle depends on the scattering of X-rays electrons surrounding atoms of the target material. For this study, XRD exhibited diffraction peaks at 2θ=25.4° for (002) plane, 2θ=43.3° for (100) and 56° for (004) are characteristic of amorphous carbon in which the characteristic peak at 2θ=43.3° is associated with the electrical conductivity of carbon materials. Composite of Co_3O_4/Ac showed distinguished diffraction peaks at 18.9,31.5, 36.3, 37.6, 43.1, 55.3, 58.7 and 62.6^o which is associated to (111), (220), (311), (222), (400), (422), (511) and (440) planes of cubic Joint Committee on Powder Diffraction Standards *(JCPD78-1970*) (Veeramani *et al.*, 2017a). They show similarity to that of the pure Co_3O_4 but relatively less crystalline in nature because of amorphous carbon (Xie *et al.*, 2013). On the contrary titanium dioxide/carbon diffraction peaks were observed at 25.2° (1 0 1), 38.0° (004), 48.1° (2 0 0), 54.0° (105), 54.9° (2 1 1), 62.7° (204), 68.7°(116) and 70.2° (2 2 0), signifying availability of anatase TiO_2 in the composite (crystallographic JCPDS card no. 21-1272) (Kim and Park, 2017). Though without the main diffraction peak of porous carbon at 26° (002) probably because of the overlap with (101) peak of anatase TiO_2 (Xiao *et al.*, 2016). X-Ray diffraction spectra of Co_3O_4/TiO_2/Ac composite showed many broad peaks

with an obvious broad peak at 26.5º, which corresponds to the (002) crystal plane of porous carbon. Broad diffraction peaks at 2θ= 37.4° (311), 55.7° (422), 59.4° (511) and 65.2° (440) may be associated with the cubic phase of Co_3O_4 that match with standard JCPDS card no-42-1467. Diffraction peaks at 2θ= 68° (116) are associated to anatase TiO_2 which usually has a pronounced peak located at 25.6 (101) that happens to overlap with diffraction peak of carbon located at 25.4 (002). This kind of peaks validates the formation of the composites. It should be noted that poor crystallinity is associated to low lattice energy, and therefore an advantage to electrode materials because of the easy de-intercalation process that contributes to the observed superior electrochemical performance (Kadam *et al.*, 2018b).

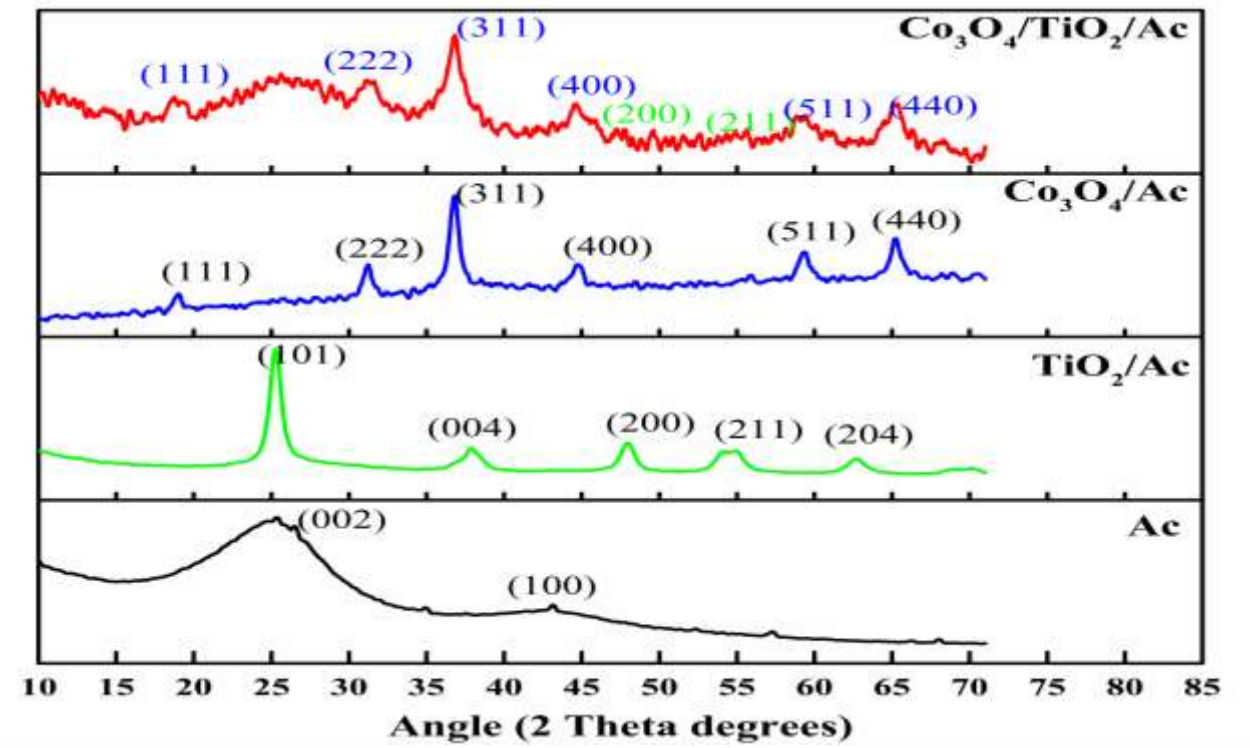

Figure 6: XRD patterns of Co_3O_4/TiO_2/Ac, Co_3O_4/Ac, /TiO_2/Ac and Ac active materials.

4.3 Morphological studies

Field emission scanning electron microscope (FE-SEM) is an instrument which gives information on the shape and structure of the material under investigation. Figure 7 shows FE-SEM images of porous carbon and composites. It demonstrates that all the samples are composed of porous surface built by irregular channels. Specifically, Fig. 7(a) shows triangular-shaped structures uniformly distributed while Fig. 7(b) shows TiO_2 as white agglomerates well dispersed in porous carbon. Cobalt oxide/carbon composite in Fig. 7(c)

shows small pores distributed on the surface with irregular compacted particles. Figure 7(d) shows cobalt/titania/carbon composite having highly interconnected pores with black spots in the pores which may aid in mass transport of electrolyte ions during charging and discharging processes of electrode material (Gong *et al.*, 2016).

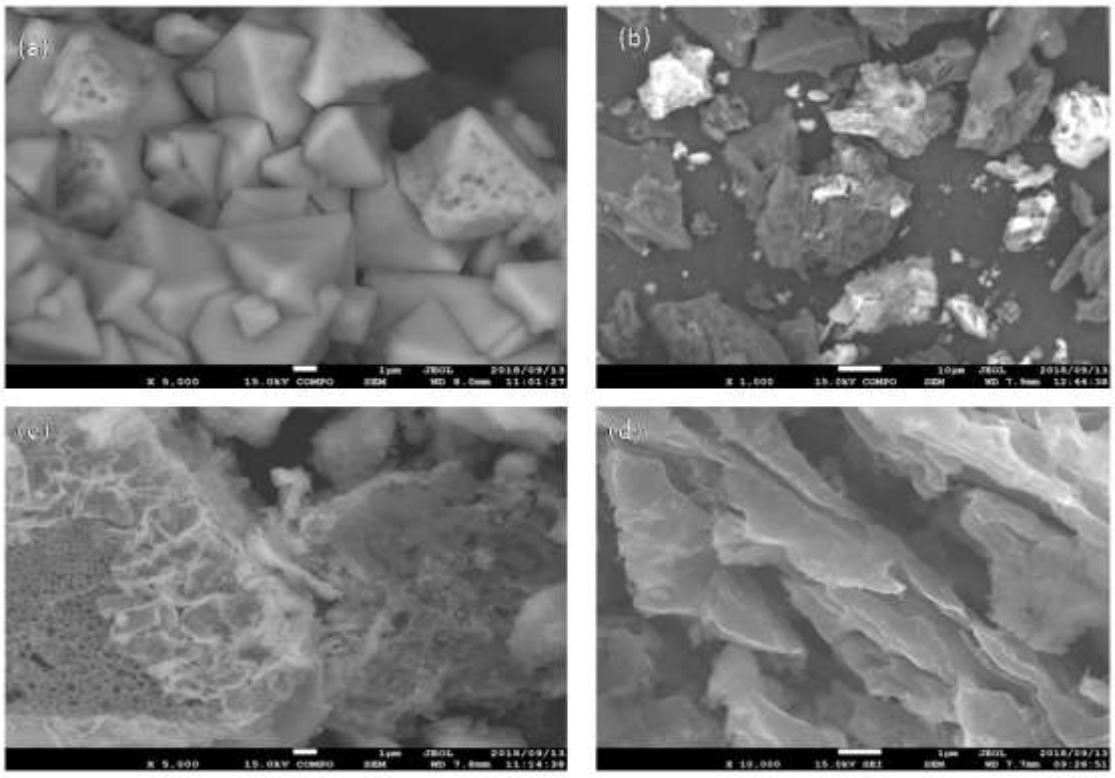

Figure 7: SEM images of carbon and composites (a) Ac, (b) TiO_2/Ac (c) Co_3O_4/Ac and (d) $Co_3O_4TiO_2$/Ac.

4.4 Nitrogen adsorption-desorption analysis

In order to quantify porosity of the electrodes, N_2 adsorption-desorption isotherms were determined for powder Co_3O_4/TiO_2/Ac as manifested in Fig. 8. The calculated BET specific surface area of the composite was 13.87 $m^2 g^{-1}$ while the average pore size of the composite was 19.74 nm, a clear indication that the sample had plenty of large mesopores. The composite exhibits a typical type-IV isotherm with a H2 hysteresis loop at P/P_0 = 0.5-1.0, samples exhibited H2 type stipulating that the pores assumed channel-like orientation corresponding to large mesopores. On the contrary, at a pressure range between P/P_0 = 0–0.4, the curve showed almost negligible adsorption volume, probably because of the low number of micropores. Figure 8 (b) shows different sizes of pores are well distributed in a unique

trimodal structure composed of small mesopores (with a peak value of 3.2 nm), medium mesopores (with a peak value of 9.1 nm and large mesopores (with a peak value of 26.1 nm). Figure 8 (c) shows cumulative pore volume of the sample, it displays that the total pore volume is 0.057 cm^3 g^{-1} contributed by only mesopores. Just like the isotherm and pore size distribution plots, cumulative pore volume indicates the absence of micropores and presence of a wide range of mesopores. It is worth mentioning that this wide range of small to large mesopores are available for storage of ions and provision of a clear pathway at which electrolytes can easily diffuse in the material and therefore very important in practical applications of a supercapacitor.

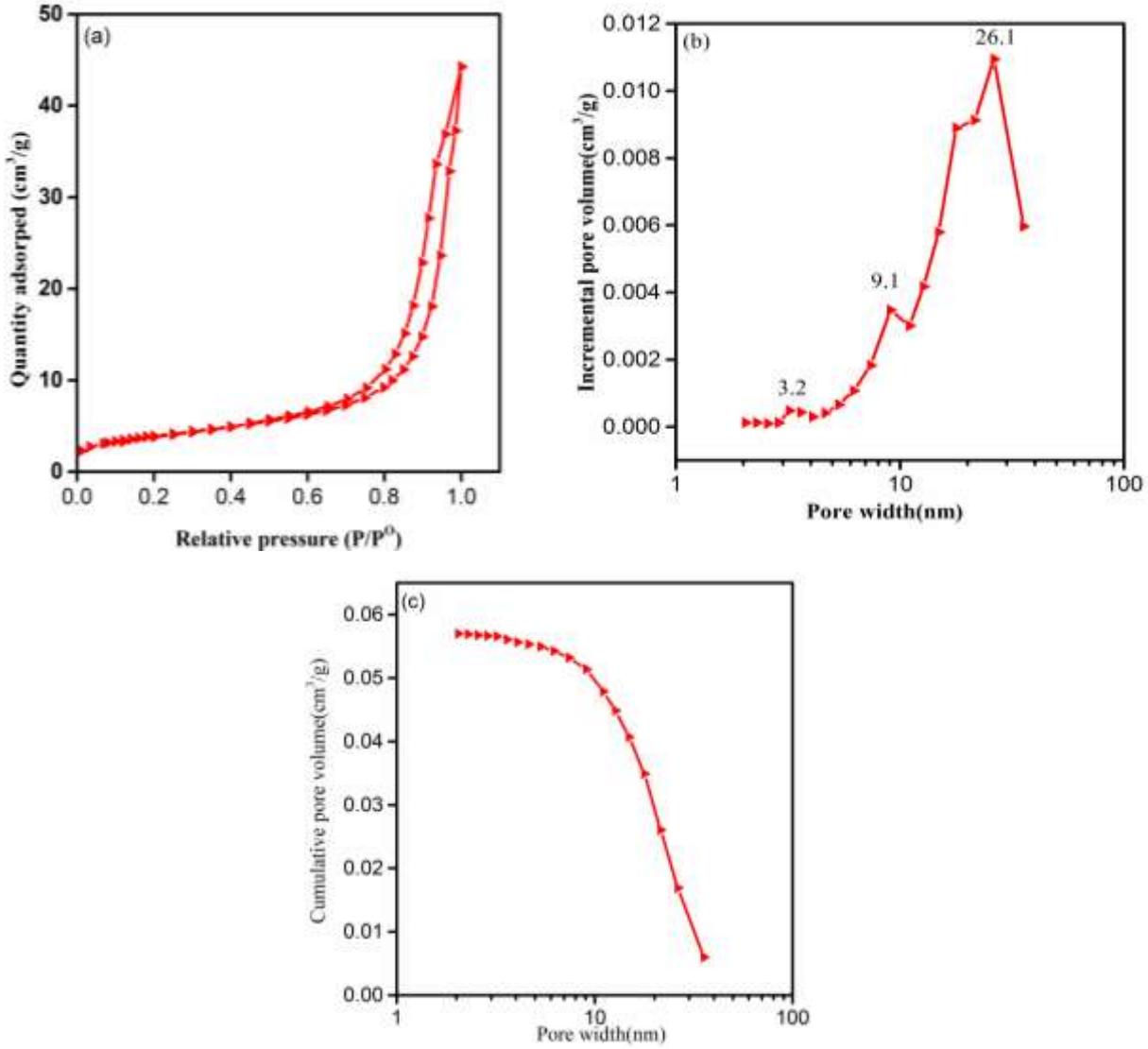

Figure 8: (a) Nitrogen adsorption/desorption isotherm (b) Pore size distribution and (c) Cumulative pore volume for Co_3O_4/TiO_2/Ac composite.

4.5 Fourier-transform infrared spectroscopy measurements

The surface chemistry of electrode materials has shown a huge difference in performance and therefore Fourier-transform infrared (FT-IR) spectroscopy was important in determining available functional groups. For porous carbon materials, the broad FT-IR peak observed at 3452 cm^{-1} is related to the vibration of hydrogen-bonded O-H stretching vibrations, then –COOH was assigned to 1639 cm^{-1} and C-O was assigned to 1382 cm^{-1}. Availability of oxygen-containing functional groups, like hydroxyl and carbonyl groups can react with the electrolyte ion to initiate pseudo-capacitance. Pseudo-capacitance can significantly improve the electrical conductivity and generally improves specific capacitance value of porous carbon.

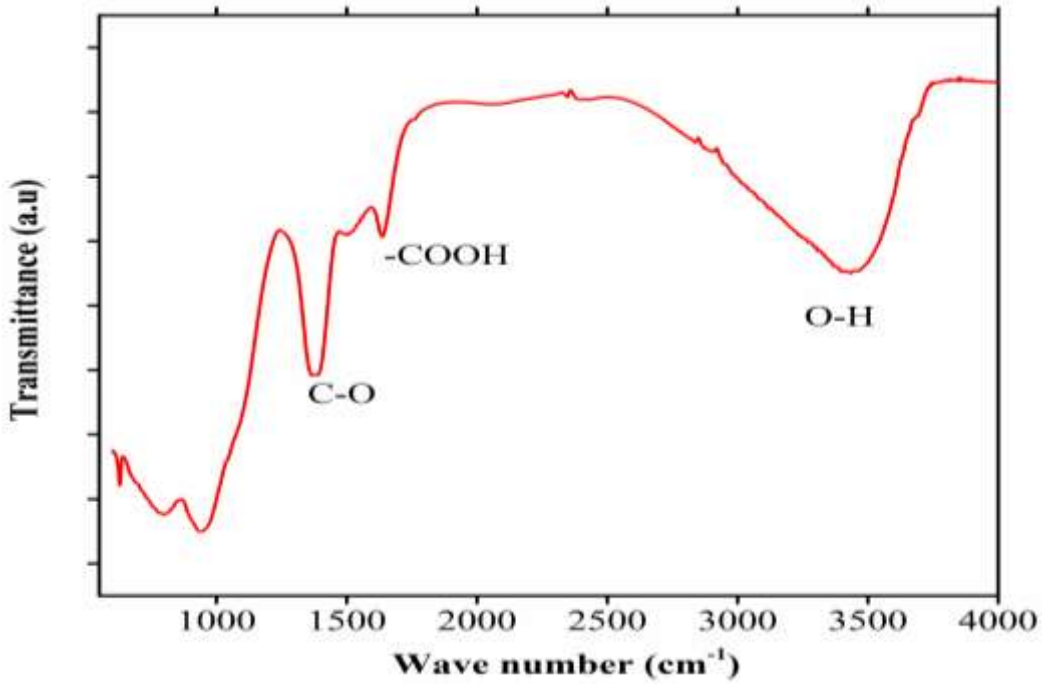

Figure 9: FT-IR spectra of porous carbon

4.6 Electrochemical measurements

Cyclic voltammetry (CV) measurements of active material were evaluated over a standard three-electrode cell system in 6 M KOH electrolyte scanning from 5 - 150 mV s^{-1}. Figure 10 (a) shows an electrical double layer property that slightly deviates from the rectangular capacitive shape probably because of the presence of impurities in carbon framework that induce pseudocapacitive properties. It is observed that when there is an increase in a potential

scan, the electrode oxidation peak tend to move towards the positive direction while the reduction peak moves in the negative direction. This might be because of the increasing resistance towards higher scan rates.

The CV curves of Fig. 10 (b), (c) and (d) show the presence of redox peaks even at a higher scan rate which indicates not only the pseudocapacitive nature of electrode material but also demonstrates the good rate capacity of the electrodes (Kadam *et al.*, 2018b). With exception to porous carbon which performed better in the negative window (-1 to -0.1), all other composites exhibited higher specific capacitance in the positive potential window though their operational window was confined at 0.5 V because the current increased sharply on scanning beyond 0.52 V. This phenomenon was due to hydrolysis of water in the aqueous electrolyte releasing oxygen bubbles and therefore confining this voltage window at 0.5 V (Sahoo and Satpati, 2017).

Pairs of redox peak revealed that faradaic redox reactions of both Co_3O_4 and TiO_2 are the main sources of energy in the electrodes. The composite electrode possesses beneficial properties of a supercapacitor as evidenced from the increase in pseudocapacitive current as well as the observed steady shift of the oxidation peaks towards higher overpotentials and reduction peak towards lower overpotentials when the scan rate is increased (Veeramani *et al.*, 2017b). Cobalt oxide loses electrons (oxidation) in presence of alkaline electrolyte at the anodic peak because of the following two processes as shown in equations 4 and 5 (Kadam *et al.*, 2018a).

$$Co_3O_4 + H_2O + OH^- \rightleftharpoons 3CoOOH + e^- \tag{4}$$

$$CoOOH + OH \rightleftharpoons CoO_2 + H_2O + e^- \tag{5}$$

Contrary to Co_3O_4, TiO_2 in Co_3O_4/TiO_2/Ac composite shows titanium atoms changing from one oxidation number to another in the presence of alkali cations (K^+) as expressed in equations below (Zhang *et al.*, 2017a).

$$TiO_2 + 2H_2O + e^- \rightleftharpoons Ti(OH)_3 + OH^- \tag{6}$$

$$xK^+ + yTiO_2 + e^- \rightleftharpoons K_x(TiO_2)y \tag{7}$$

The specific capacitance of Co_3O_4/TiO_2/Ac is higher than other active materials as evidenced by the large integral area of the cyclic voltammogram in Fig 11. Since nickel foam does not show a significant contribution to the displayed specific capacitance in the voltage windows between 0 to 0.5 V, this, therefore, means that the high supercapacitive performance may be assigned to the synergistic effects of individual materials. Cobalt oxide may have contributed to this high capacitance because of its good pseudocapacitive property. On the other hand, carbon improved the wettability and significantly reduced electrical resistance in the composite while TiO_2 may have contributed to this electrochemical performance because of the effect of single-direction polarity. Titanium dioxide nanoparticles have a high concentration of charges on their surface and this reduces polarization on Ac electrodes increasing the movement of ions in the porous carbon leading to an improved specific capacitance of the entire composite (Seo and Park, 2010).

The difference in operation voltages in Fig for transition metal oxide composites electrode (0-0.5 V) and for carbon electrode (-0.9 - 0.0 V) indicates a practical match of both voltage windows of the electrode materials. Therefore, the operation voltages show that they have the capability to expand up to 1.4 V using the maximum voltage of composites (0.5 V) and a minimum voltage window of Ac (0.9 V).

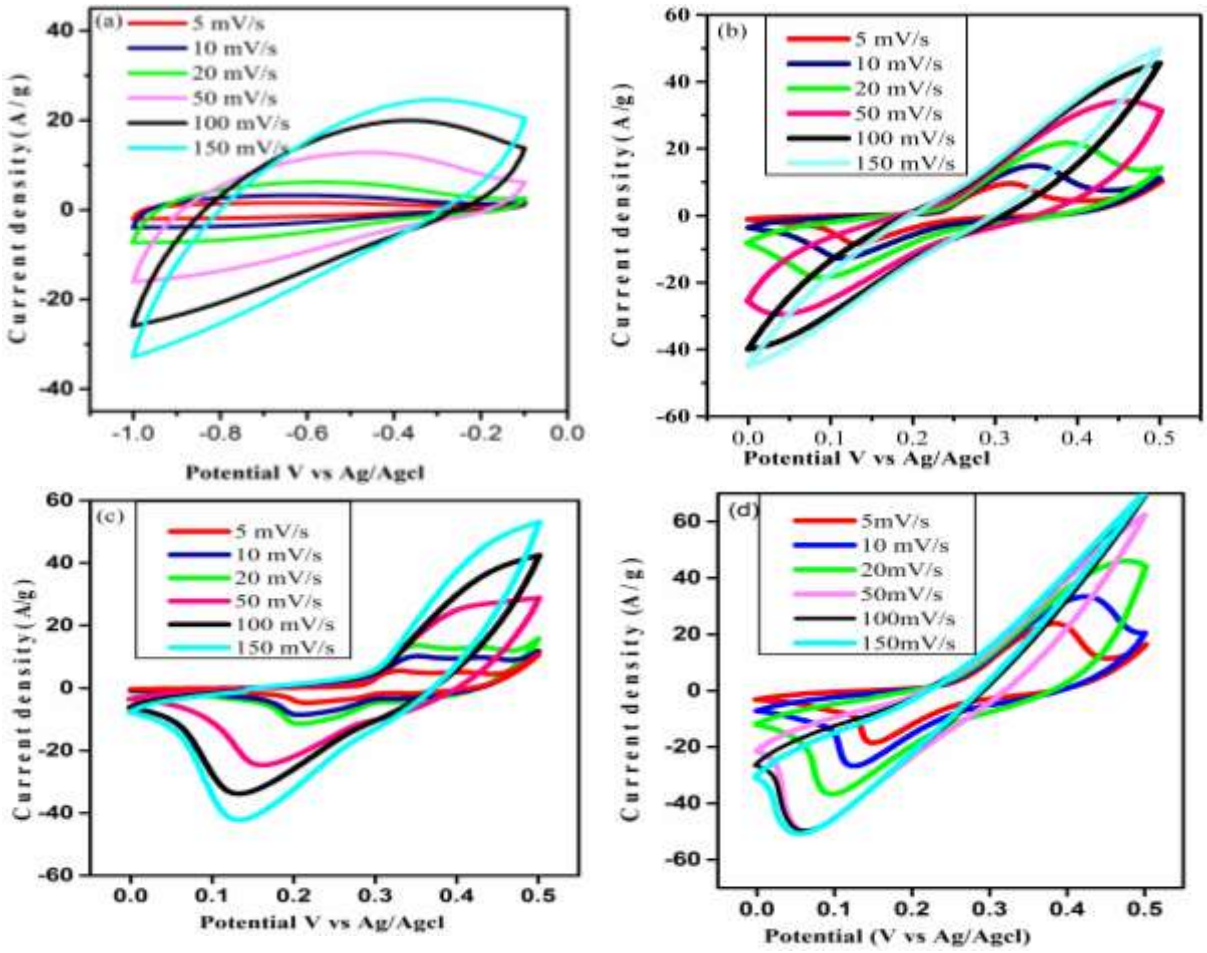

Figure 10: Cyclic voltammogram of (a) Ac (b) TiO_2/Ac, (c) Co_3O_4/Ac and (d) Co_3O_4/TiO_2/Ac in 6 M KOH solution at different scanning rates.

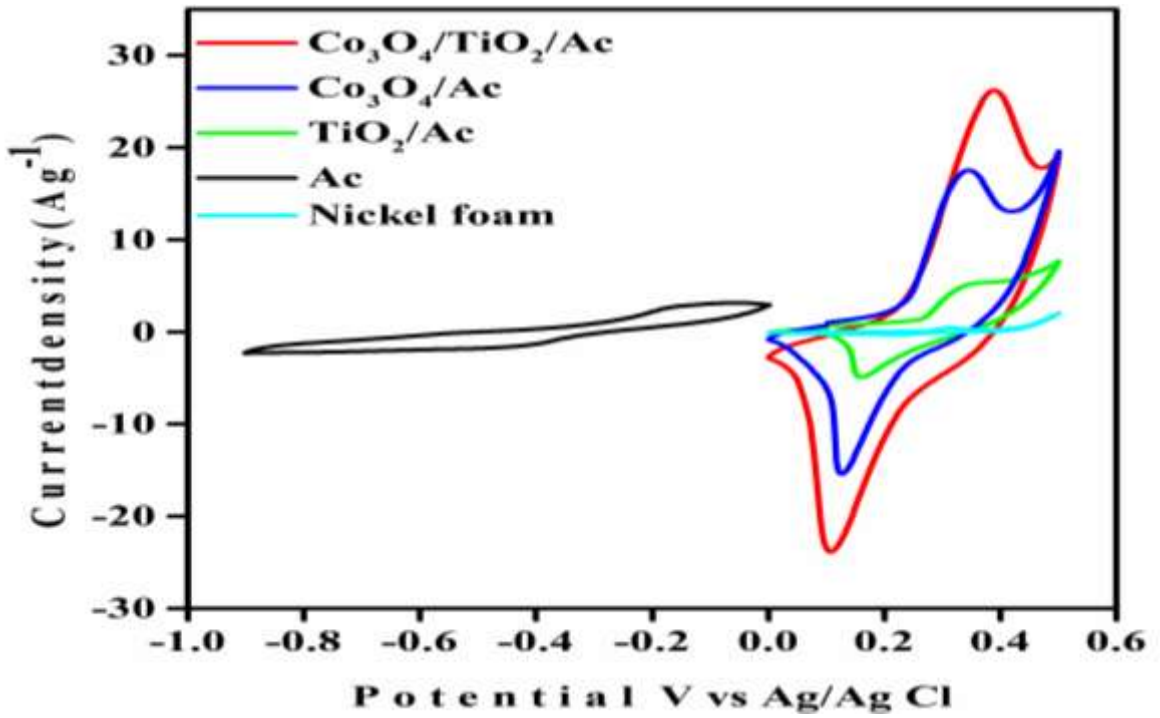

Figure 11: Cyclic voltammogram of Co_3O_4/TiO_2/Ac, Co_3O_4/Ac, TiO_2/Ac, and Ac at a scanning rate of 5 mV s^{-1}.

The best specific capacitance obtained for Co_3O_4/TiO_2/Ac was 946 Fg^{-1}, higher than 845 F g^{-1} for Co_3O_4/Ac, 340 F g^{-1} for TiO_2/Ac and 308 F g^{-1} for Ac at a scan rate of 5 mV s^{-1}. This high capacitance might be because of synergistic effects. Figure 12(a) shows that all electrodes display a similar trend of higher specific capacitances at lower scan rate and vice versa. This is probably because, at lower scan rate the electrolyte ions had full access to the internal part of the electrode material resulting into a total utilization of the electrode material. Contrary to low scan rate, at higher scan rate, ions in electrolytes can only interact partially (mostly on the surface) with the active material hence displaying low specific capacitance (Kadam *et al.*, 2018b).

To evaluate the practical applications of these materials, cyclic voltammetry was used at 30 mV s^{-1} for 2000 cycles in concentrated 6 M KOH solution. All electrodes showed a general drop in specific capacitance after 2000 cycles as depicted in Fig. 12(b) where Co_3O_4/TiO_2/Ac, Co_3O_4/Ac, TiO_2/Ac, and Ac exhibited a retention capacity of 87.7%, 83.3%, 90.6% and 97.5%, respectively. This drop of capacitance may arise because most materials either dissolve in electrolytes or fall off from the electrode during early cycling (Kadam *et al.*, 2018b). Porous carbon showed superior cycle stability more than composites. This

excellent stability is among the most attractive properties of carbon materials given that they do not undergo chemical reactions during cycling. It is important to also state that stability of carbon can be improved further by the presence of impurities such as heteroatom doped in the carbon framework. Though composites of transition metal oxides and carbon showed pronounced capacity fading, this is because they undergo structural change and volume expansion during cycling (Guan *et al.*, 2017). Contrary to other electrode materials, TiO_2/Ac electrode interestingly exhibits better stability than other composites. This difference can be ascribed to the fact that titanium dioxide as a transition metal oxide experiences comparatively lower volume expansion during cycling (Zhang *et al.*, 2017a).

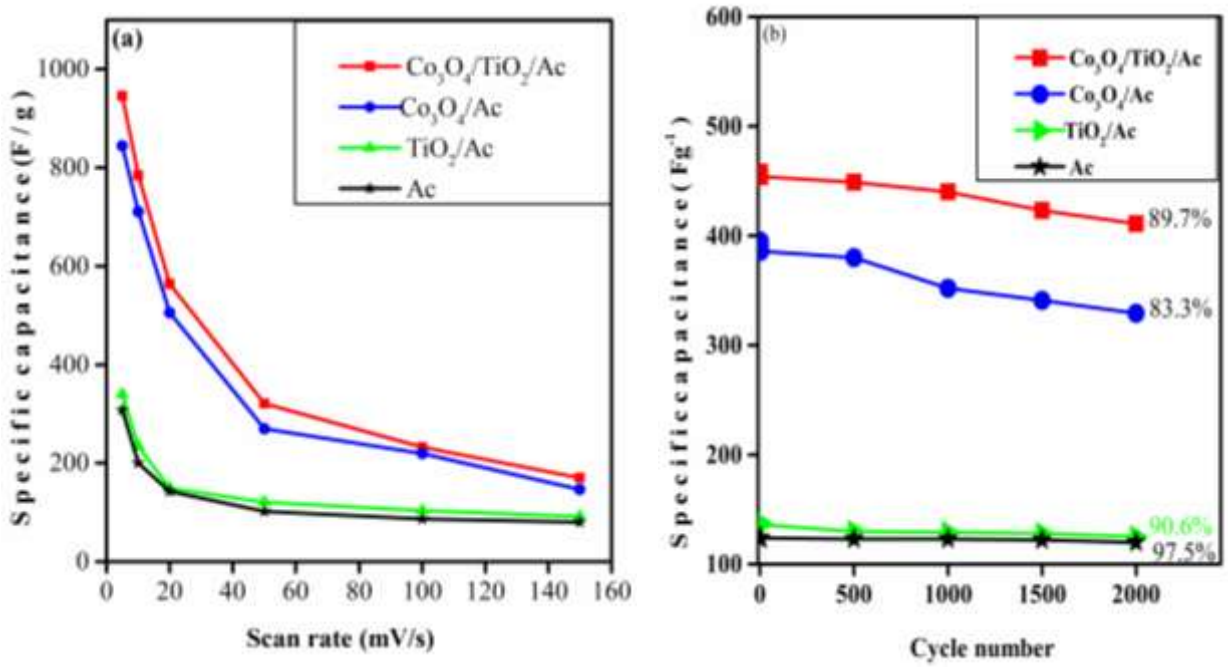

Figure 12: Specific capacitance vs. scan rate of (a) and (b) Cyclic stability of Ac, TiO_2/Ac, Co_3O_4/Ac, and Co_3O_4/TiO_2/Ac in 6 M KOH**.**

Figure 13 (a) shows Nyquist plots of the electrode material, which mainly have three parts. A semicircle in the high-frequency region that represents the interfacial charge transfer resistance between the electrode and the electrolyte. A slanting line approximately 45° in the low-frequency region and a straight line with a slope larger than 45° in the very low-frequency region (Xia *et al.*, 2018). The real part (Z') in the high-frequency region represents the total resistance known as equivalent series resistance (ESR) of both electrolyte and electrode. Porous carbon (Ac), Co_3O_4/Ac, Co_3O_4/TiO_2/Ac, and TiO_2/Ac exhibited resistances of 0.5 Ω, 0.52 Ω, 0.6 Ω and 1.1 Ω respectively indicating that both the electrolyte and

electrode material have good electrical conductivity. In the very low-frequency region, Ac showed an almost vertical line along the imaginary axis revealing electrochemical properties close to ideal capacitive behavior (Tajik *et al.*, 2017). Composites (Co_3O_4/TiO_2/Ac, Co_3O_4/Ac, and TiO_2/Ac) showed more inclined curves suggesting the presence of pseudocapacitance (Guo *et al.*, 2018). Charge transfer resistance, ESR, related to faradaic reactions can be obtained from the diameter of a semicircular arc but in our case, the semicircular arc is very small, similar to the reported results (Wang and Zhang, 2017), meaning that the ESR is rather small. This can be attributed to the following: hydrophilic nature of titania which has an advantage of excellent ion transportation (Patil *et al.*, 2018), improved wettability because of surface oxygen-containing functional groups, pressing of active electrode material as researchers interestingly argue that the application of mechanical pressure after loading can reduce the ESR by 90% and increase the capacitance by 128% due to a decrease in the thickness of the diffusion layer (Li *et al.*, 2015). Lastly, the availability of large mesopores that acted as reservoirs for charges and provided easy transportation of electrolytes, hence improved electrochemical performance.

Bode plot results shown in Fig. 13(b) complements Nyquist plots of Fig. 13(a). Generally conventional capacitors show resistive behavior at high frequencies and capacitive behavior at low frequencies when θ approaches –90°. Capacitor response times (τ_0) can be calculated from the frequency when θ = -45°, this is the frequency at which the resistive and capacitive impedances are the same. Ac exhibits better capacitive properties with an angle of -76° close to -90° whereas the composites (Co_3O_4/Ac, Co_3O_4/TiO_2/Ac, and TiO_2/Ac) showed comparable phase angles of -64°,-56° and -51°, respectively. These angles are closer to -45° probably because of the introduction of transition metal oxides in the porous carbon (Karthik *et al.*, 2017). Characteristic frequencies f_0 at 45° were 4.0, 1.0, 0.45 and 0.28 Hz for Ac, Co_3O_4/TiO_2/Ac, Co_3O_4/Ac and TiO_2/Ac electrodes, respectively, corresponding to the characteristic response time (τ_0) of 0.25, 1.0, 2.2 and 3.6 s. Such short response times for active material in 6 M KOH electrolyte may be a reason for their high power delivery.

Generally, Fig. 13(d) shows that all active materials display a similar trend of an increase in specific capacitance with a decrease in the frequency at the high-frequency region. The Co_3O_4/TiO_2/Ac composite electrode exhibited much lower specific capacitance than Co_3O_4/Ac, TiO_2/Ac and Ac electrodes between 0.1 to 10 Hz frequency range and exhibited

higher capacitance when approaching frequency 0.01. This trend is probably because, at higher frequencies, the electrolyte ions could not fully have an access of the inner part of the electrodes but rather only the outer surface of active material could be utilized for faradaic reactions and charge storage leading to low specific capacitance. At low frequency, the electrolyte seeps deep in the electrode material utilizing a bigger percentage of the surface of the material hence significantly improving faradaic reactions (charge storage) and therefore displaying the observed high capacitance value.

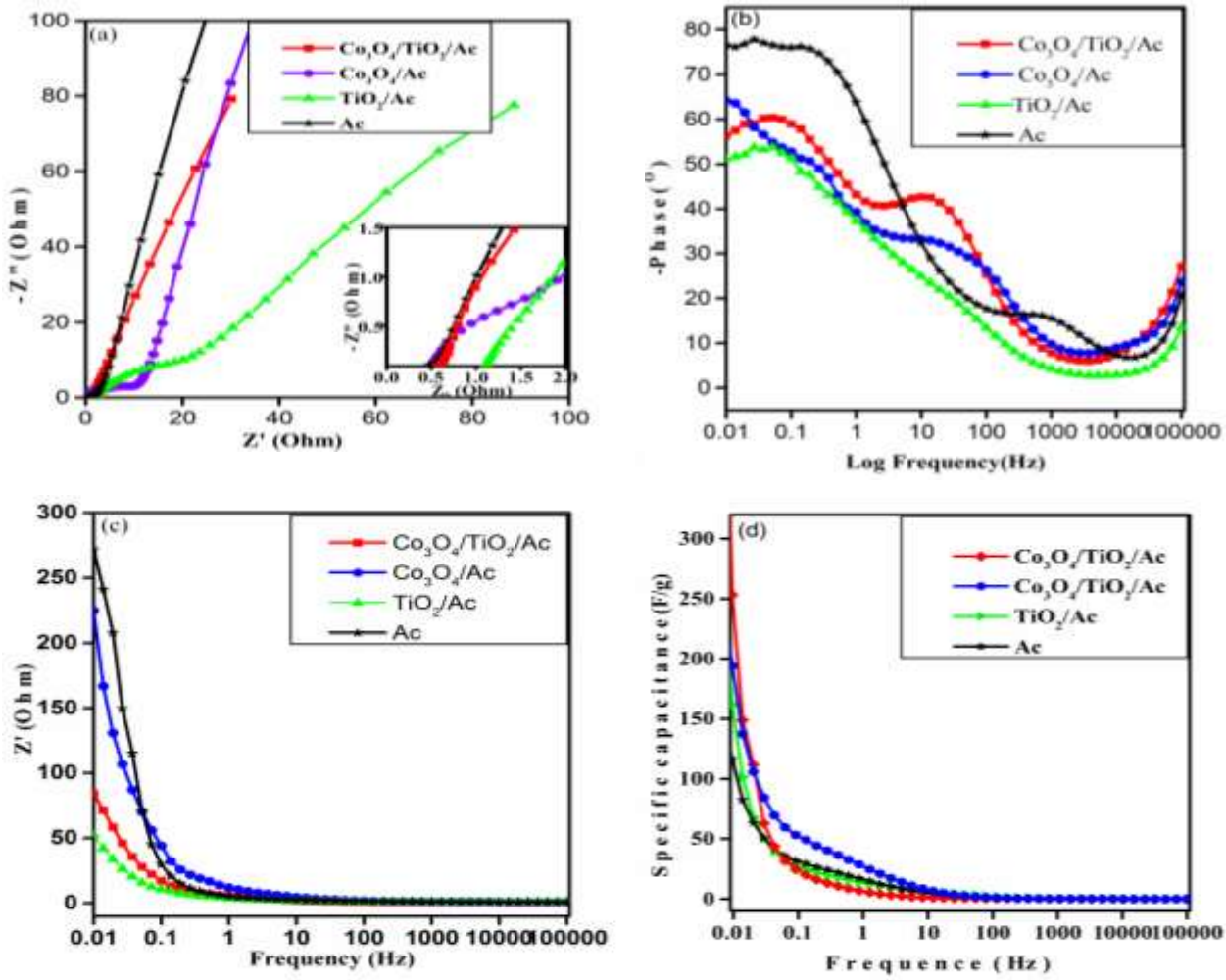

Figure 13: Nyquist plots (a) and bode plots (b, c and d) –phase angles, real impedance and specific capacitance as a function of frequency of all electrodes respectively in 6 M KOH.

CHAPTER FIVE

CONCLUSION AND RECOMMENDATIONS

5.1 Conclusion

In this study, fish bladder derived carbon was prepared via carbonization followed by KOH activation. Composites of Co_3O_4/TiO_2/Ac, Co_3O_4/Ac, and TiO_2/Ac were synthesized via simple sol-gel method prior heat treatment. The specific capacitance of Co_3O_4/TiO_2/Ac was 946 F g^{-1} as compared to Co_3O_4/Ac, TiO_2/Ac, and Ac with specific capacitances of 845 F g^{-1}, 340 F g^{-1} and 308 F g^{-1}, respectively. This study showed that low energy density associated with supercapacitor application can be solved by a combination of cheaply available materials with less toxic transition metal oxides if the chemistry among the materials involved is well understood and optimized for the benefit of the society. Cycle life was evaluated using cyclic voltammetry, Co_3O_4/TiO_2/Ac, Co_3O_4/Ac, TiO_2/Ac, and Ac shows specific capacity retention of 89.7%, 83.3%, 90.6% and 97.5%, respectively, after 2000 cycles at 30 mV s^{-1}.

Impedance spectroscopy revealed that the materials had good conductivity as evidenced by their low series resistance of 0.5 Ω, 0.52 Ω, 0.6 Ω and 1.1 Ω for Ac, Co_3O_4/Ac, Co_3O_4/TiO_2/Ac, and TiO_2/Ac, respectively. This study demonstrated that Co_3O_4/TiO_2/Ac is an experimental electrode material with the ability to meet demands for practical application in the next generation. Moreover, this route opens an avenue for the synthesis of different electrochemical materials and allows facile scale-up to form carbon-based composites for future commercial applications.

5.2 Recommendations

To commercialize supercapacitor, there is a need to maximize a wide range of factors. The following are recommendations for future work.

(i) Charge and discharge was not possible with PGSTAT204 because of the low current and therefore future work should consider this technique to determine the columbic efficiency, power density, and energy density

(ii) Higher mass loading approximately 10 mg should be considered in order to realize commercial application in the field of a supercapacitor.

(iii) Potassium electrode was used as an electrolyte was used in this study because of its safety, affordability, low inflammability and high lifetime. However, the range of working potential window is limited to approximately 1 V. Future studies should consider developing and testing performance of synthesized electrodes in different electrolytes.

(iv) Fish bladder derived carbon as one of the material in the composite performed well but we recommend that future research should vary other parameters like temperature used for carbonization and activation as well as the ratio of KOH: carbon so as to evaluate their effects.

(v) The method employed was the sol-gel synthesis, which requires binders to make electrodes. We would wish to recommend binder-free methods that will probably afford higher capacitance than the one reported in this study.

REFERENCES

Achour, A., Chaker, M., Achour, H., Arman, A., Islam, M., Mardani, M., . . . Brousse, T. (2017). Role of nitrogen doping at the surface of titanium nitride thin films towards capacitive charge storage enhancement. *Journal of Power Sources*. **359**, 349-354. doi: 10.1016/j.jpowsour.2017.05.074.

Aghazadeh, M., Bahrami, A., Gharailou, D., Maragheh, M. G., Ganjali, M. R., & Norouzi, P. (2016). Mn_3O_4 nanorods with secondary plate-like nanostructures; preparation, characterization and application as high performance electrode material in supercapacitors. *Journal of Materials Science: Materials in Electronics*. **27**(11), 11192-11200. doi: 10.1007/s10854-016-5239-1.

Aloo, P. A., Njiru, J., Balirwa, J. S., & Nyamweya, C. S. (2017). Impacts of Nile Perch, Lates niloticus, introduction on the ecology, economy and conservation of Lake Victoria, East Africa. *Wiley Interdisciplinary Reviews: Systems Biology and Medicine*. **22**, 1-14. doi: doi: 10.1111/lre.12192.

An, C., Wang, Y., Jiaob, L., & Yuan, H. (2016). Mesoporous Ni@C hybrids for a high energy aqueous asymmetric supercapacitor device. *Journal of Material Chemistry A*. **3**(4), 9670-9676 doi: 10.1039/C6TA02339H10.1039.

Anilkumar, K., Manoj, M., Jinisha, B., Pradeep, V., & Jayalekshmi, S. (2017). Mn_3O_4/reduced graphene oxide nanocomposite electrodes with tailored morphology for high power supercapacitor applications. *Electrochimica Acta*. **236**, 424-433. doi: doi.org/10.1016/j.electacta.2017.03.167.

Ansari, S. A., Fouad, H., Ansari, S. G., Sk, M. P., & Cho, M. H. (2017). Mechanically exfoliated MoS_2 sheet coupled with conductive polyaniline as a superior supercapacitor electrode material. *Journal of Colloid and Interface Science*. **504**, 276-282. doi: 10.1016/j.jcis.2017.05.064.

Aradilla, D., Gao, F., Lewes, G., Müller, W., Gentile, P., Pouget, S., . . . Bidan, G. (2017). Powering electrodes for high performance aqueous micro-supercapacitors: Diamond-

coated silicon nanowires operating at a wide cell voltage of 3 V. *Electrochimica Acta*. **242**, 173-179. doi: 10.1016/j.electacta.2017.04.102.

Asen, P., Shahrokhian, S., & Zad, A. I. (2018). Ternary nanostructures of Cr_2O_3/graphene oxide/conducting polymers for supercapacitor application. *Journal of Electroanalytical Chemistry*. **823**, 505-516. doi: 10.1016/j.jelechem.2018.06.048.

Atchudan, R., Edison, T. N., Perumal, S., & Lee, Y. R. (2017). Green synthesis of nitrogen-doped graphitic carbon sheets with use of Prunus persica for supercapacitor applications. *Applied Surface Science*. **393**, 276-286. doi: 10.1016/j.apsusc.2016.10.030.

Bao, L., Zang, J., & Li, X. (2011). Flexible Zn_2SnO_4/MnO_2 core/shell nanocable− carbon microfiber hybrid composites for high-performance supercapacitor electrodes. *Nano Letters*. **11**(3), 1215-1220. doi: doi.org/10.1021/nl104205s.

Baraia, H. R., Rahmanb, M. M., & Joo, S. W. (2017). Template-free synthesis of two-dimensional titania/titanate nanosheets as electrodes for high-performance supercapacitor applications. *Journal of Power Sources*. **372**, 227-234. doi: 10.1016/j.jpowsour.2017.10.076.

Bing , L., Dai, F., Xiao, Q., Yang, L., Shen, J., Zhang, C., & Cai, M. (2016). Nitrogen-doped Activated Carbon for High Energy Hybrid Supercapacitor. *Energy and Environmental Science*. **9**, 102-106. doi: 10.1039/C5EE03149D10.1039D.

Cai, T., Wang, H., Jin, C., Sun, Q., & Nie, Y. (2017). Fabrication of nitrogen-doped porous electrically conductive carbon aerogel from waste cabbage for supercapacitors and oil/water separation. *Journal of Materials Science: Materials in Electronics*. **29**(5), 4334-4344. doi: 10.1007/s10854-017-8381-5.

Cakici, M., Kakarla, R. R., & Fernando, A. (2017). Advanced electrochemical energy storage supercapacitors based on the flexible carbon fiber fabric-coated with uniform coral-like MnO_2 structured electrodes. *Chemical Engineering Journal*. **309**, 151-158. doi: 10.1016/j.cej.2016.10.012.

Chen, G., Guan, H., Dong, C., & Wang, Y. (2018). Synthesis of core-shell carbon sphere@ nickel oxide composites and their application for supercapacitors. *Ionics*. **24**(2), 513-521. doi: https://doi.org/10.1007/s1158.

Chen, S., Cai, D., Yang, X., Chen, Q., Zhan, H., Qu, B., & Wang, T. (2017). Metal-Organic Frameworks Derived Nanocomposites of Mixed-Valent MnO^{x} Nanoparticles In-Situ Grown on Ultrathin Carbon Sheets for High-Performance Supercapacitors and Lithium-Ion Batteries. *Electrochimica Acta*. **256**, 63-72. doi: 10.1016/j.electacta.2017.10.016.

Chen, Y., Zhang, X., Zhang, D., Yu, P., & Ma, Y. (2011). High performance supercapacitors based on reduced graphene oxide in aqueous and ionic liquid electrolytes. *Carbon*. **49**(2), 573-580. doi: 10.1016/j.carbon.2010.09.060.

Chen, Y., Zhang, X., Zhang, H., Sun, X., Zhang, D., & Ma, Y. (2012). High-performance supercapacitors based on a graphene–activated carbon composite prepared by chemical activation. *RSC Advances*. **2**(20), 7747-7753. doi: 10.1039/C2RA20667F.

Cheng, P., Gao, S., Zang, P., Yang, X., Bai, Y., Xu, H., . . . Lei, Z. (2015). Hierarchically porous carbon by activation of shiitake mushroom for capacitive energy storage. *Carbon*. **86**, 158-167. doi: 10.1016/j.carbon.2015.05.056.

Cheng, P., Li, T., Yu, H., Zhi, L., Liu, Z., & Lei, Z. (2016). Biomass-Derived Carbon Fiber Aerogel as a Binder-Free Electrode for High-Rate Supercapacitors. *The Journal of Physical Chemistry C*. **120**(4), 2079-2086. doi: 10.1021/acs.jpcc.5b11280.

Chmiola, J., Yushin, G., Gogotsi, Y., Portet, C., Simon, P., & Taberna, P. L. (2006). Anomalous Increase in Carbon Capacitance at Pore Sizes Less Than 1 Nanometer. **313**(5794), 254-261. doi: 10.1126/science.1127826.

Crosnier, O., Nicolas, G., Buvat, G., Athouël, L., Douard, C., Lannelongue, P., . . . Brousse, T. (2018). Polycationic oxides as potential electrode materials for aqueous-based electrochemical capacitors. *Current Opinion in Electrochemistry*. **9**, 87-94. doi: 10.1016/j.coelec.2018.05.005.

Cui, J., Xi, Y., Chen, S., Li, D., She, X., Sun, J., . . . Guo, S. (2016). Prolifera-Green-Tide as Sustainable Source for Carbonaceous Aerogels with Hierarchical Pore to Achieve Multiple Energy Storage. *Advanced Functional Materials*. **26**(46), 8487-8495. doi: 10.1002/adfm.201603933.

Deng, X., Zhao, B., Zhu, L., & Shao, Z. (2015). Molten salt synthesis of nitrogen-doped carbon with hierarchical pore structures for use as high-performance electrodes in supercapacitors. *Carbon*. **93**, 48-58. doi: 10.1016/j.carbon.2015.05.031.

Deokate, R. J., Kalubarme, R. S., Park, C., & Lokhande, C. D. (2017). Simple Synthesis of $NiCo_2O_4$ thin films using Spray Pyrolysis for electrochemical supercapacitor application. *Electrochimica Acta*. **224**, 378-385. doi: 10.1016/j.electacta.2016.12.034.

Du, J., Zhou, G., Zhang, H., Cheng, C., Ma, J., Wei, W., . . . Wang, T. (2013). Ultrathin porous $NiCo_2O_4$ nanosheet arrays on flexible carbon fabric for high-performance supercapacitors. *Applied Material and Interfaces*. **5**(15), 7405−7409. doi: 10.1021/am4017335.

Duraisamy, N., Numan, A., Fatin, S. O., Ramesh, K., & Ramesh, S. (2016). Facile sonochemical synthesis of nanostructured NiO with different particle sizes and its electrochemical properties for supercapacitor application. *Journal of Colloid and Interface Science*. **471**, 136-144. doi: 10.1016/j.jcis.2016.03.013.

Edison, J. I., Atchudan, R., & Lee, Y. R. (2018a). Binder-free electro-synthesis of highly ordered nickel oxide nanoparticles and its electrochemical performance. *Electrochimica Acta*. **283**, 1609-1617. doi: 10.1016/j.electacta.2018.07.101.

Edison, T. N. J. I., Atchudan, R., & Lee, Y. R. (2018b). Binder-free electro-synthesis of highly ordered nickel oxide nanoparticles and its electrochemical performance. *Electrochimica Acta*. **283**, 1609-1617. doi: 10.1016/j.electacta.2018.07.101.

Enock, T. K., King'ondu, C. K., Pogrebnoi, A., & Jande, Y. A. C. (2017). Biogas-slurry derived mesoporous carbon for supercapacitor applications. *Materials Today Energy*. **5**, 126-137. doi: 10.1016/j.mtener.2017.06.006.

Fan, X., Yu, C., Yang, J., Ling, Z., & Qiu, J. (2014). Hydrothermal synthesis and activation of graphene-incorporated nitrogen-rich carbon composite for high-performance supercapacitors. *Carbon*. **70**, 130-141. doi: 10.1016/j.carbon.2013.12.081.

Fang, J., Liu, Q., Yang, S., Zhang, X., Wei, C., Tan, M., & Wen, S. (2018). Design and synthesis of N-doped mesoporous carbon@$NiCo_2O_4$ nanocomposites with various morphologies for high electrochemical performance applied in supercapacitors. *Materials Research Bulletin*. **105**, 312-317. doi: 10.1016/j.materresbull.2018.05.006.

Faraji, M., Moghadam, P. N., & Hasanzadeh, R. (2016). Fabrication of binder-free polyaniline grafted multiwalled carbon nanotube/TiO_2 nanotubes/Ti as a novel energy storage electrode for supercapacitor applications. *Chemical Engineering Journal*. **304**, 841-851. doi: doi.org/10.1016/j.cej.2016.07.034.

Fic, K., Platek, A., Piwek, J., & Frackowiak, E. (2018). Sustainable materials for electrochemical capacitors. *Materials Today*. **21**(4), 437-454. doi: 10.1016/j.mattod.2018.03.005.

Fu, G., Li, Q., Ye, J., Han, J., Wang, J., Zhai, L., & Zhu, Y. (2018). Hierarchical porous carbon with high nitrogen content derived from plant waste (pomelo peel) for supercapacitor. *Journal of Materials Science: Materials in Electronics*. **29**(9), 7707-7717. doi: 10.1007/s10854-018-8766-0.

Gnana, B., Asiri, A. M., Wu, J. J., & Anandan, S. (2015). Synthesis of Mn_3O_4 nanoparticles via chemical precipitation approach for supercapacitor application. *Journal of Alloys and Compounds*. **636**, 234-240. doi: 10.1016/j.jallcom.2015.02.164.

Gong, C., Wang, X., Ma, D., Chen, H., Zhang, S., & Liao, Z. (2016). Microporous carbon from a biological waste-stiff silkworm for capacitive energy storage. *Electrochimica Acta*. **220**, 331-339. doi: 10.1016/j.electacta.2016.10.120.

Gu, L., Wang, Y., Lu, R., Wang, W., Peng, X., & Sha, J. (2015). Silicon carbide nanowires@$Ni(OH)_2$ core–shell structures on carbon fabric for supercapacitor electrodes with excellent rate capability. *Journal of Power Sources*. **273**, 479-485. doi: 10.1016/j.jpowsour.2014.09.113.

Guan, C., Qian, X., Wang, X., Cao, Y., Zhang, Q., Li, A., & Wang, J. (2015). Atomic layer deposition of Co_3O_4 on carbon nanotubes/carbon cloth for high-capacitance and ultrastable supercapacitor electrode. *Nanotechnology*. **26**(9), 094001. doi: 10.1088/0957-4484/26/9/094001.

Guan, C., Zhao, W., Hu, Y., Lai, Z., Li, X., Sun, S., . . . Wang, J. (2017). Cobalt Oxide and N-doped Carbon Nanosheets Derived from a Single Two-Dimensional Metal–Organic Framework Precursor and their Application in Flexible Asymmetric Supercapacitors. *Royal Society of Chemistry*. **2**, 99-105. doi: 10.1039/C6NH00224B.

Guo, X., Zhang, W., Qian, C., Yang, H., & Fan, T. (2018). MnO_2/C composite with 3D hierarchical architecture for high-performance supercapacitor electrodes. *Ceramics International*. **44**(8), 9696-9702. doi: 10.1016/j.ceramint.2018.02.200.

Han, Y., Shen, N., Zhang, S., Li, D., & Li, X. (2017). Fish gill-derived activated carbon for supercapacitor application. *Journal of Alloys and Compounds*. **694**(4), 636-642. doi: 10.1016/j.jallcom.2016.10.013.

Hao, F., Yan, Y., Gao, G., Mu, S., & Hao, C. (2017). Ionothermal Synthesis of Graphene-Based Hierarchically Porous Carbon for High-Energy Supercapacitors with Ionic Liquid Electrolyte. *Electrochimica Acta*. **241**, 124-131. doi: 10.1016/j.electacta.2017.04.128.

He, H., & Li, M. (2018). Preparation of three-dimensional porous graphene/ruthenium oxide nano-composite for high performance supercapacitors by electrochemical method. *Integrated Ferroelectrics*. **189**(1), 147-157. doi: 10.1080/10584587.2018.1456181.

He, Z., Zhang, G., Chen, Y., Xie, Y., Zhu, T., Guo, H., & Chen, Y. (2016). The effect of activation methods on the electrochemical performance of ordered mesoporous carbon for supercapacitor applications. *Journal of Materials Science*. **52**(5), 2422-2434. doi: 10.1007/s10853-016-0536-x.

Hou, J., Jiang, K., Wei, R., Tahir, M., Wu, X., Shen, M., . . . Cao, C. (2017). Popcorn-Derived Porous Carbon Flakes with an Ultrahigh Specific Surface Area for Superior

Performance Supercapacitors. *ACS Applied Materials and Interfaces*. **9**(36), 30626-30634. doi: 10.1021/acsami.7b07746.

Hout, S. I., Chen, C., Liang, T., Yang, L., & Zhang, J. (2017). Cetyltrimethylammonium bromide assisted hydrothermal synthesis of cobalt oxide nanowires anchored on graphene as an efficient electrode material for supercapacitor applications. *Materials Chemistry and Physics*. **198**, 99-106. doi: 10.1016/j.matchemphys.2017.05.051.

Hu, L., Hou, J., Ma, Y., Li, H., & Zhai, T. (2016). Multi-heteroatom self-doped porous carbon derived from swim bladders for large capacitance supercapacitors. *Journal of Materials Chemistry A*. **4**(39), 15006-15014. doi: 10.1039/c6ta06337c.

Iro, Z. S., Subramani, C., & Dash, S. S. (2016). A Brief Review on Electrode Materials for Supercapacitor. *International Journal of Electrochemical Science*. **11**, 10628 – 10643. doi: 10.20964/2016.12.50.

Islam, M. S., Deng, Y., Tong, L., Faisal, S. N., Roy, A. K., Minett, A. I., & Gomes, V. G. (2016). Grafting carbon nanotubes directly onto carbon fibers for superior mechanical stability: Towards next generation aerospace composites and energy storage applications. *Carbon*. **96**, 701-710. doi: 10.1016/j.carbon.2015.10.002.

Jang, G., Ameen, S., Akhtar, M. S., Kim, E., & Shin, H. (2017). Electrochemical Investigations of Hydrothermally Synthesized Porous Cobalt Oxide (Co_3O_4) Nanorods: Supercapacitor Application. *Chemistry Select*. **2**(28), 8941-8949. doi: 10.1002/slct.201701571.

Jiao, Z., Wu, Q., & Qiu, J. (2018). Preparation and electrochemical performance of hollow activated carbon fiber - Carbon nanotubes three-dimensional self-supported electrode for supercapacitor. *Materials and Design*. **154**(6), 239-245. doi: 10.1016/j.matdes.2018.05.021.

Jing, H., Ge, J., Ren, Z., Tu, J., Sun, Z., Chen, S., & Xie, G. (2017). Facile green synthesis of 3D porous glucose-based carbon aerogels for high-performance supercapacitors. *Electrochimica Acta*. **258**(5), 951-958. doi: 10.1016/j.electacta.2017.11.146.

Jo, W., Kumar, S., Isaacs, M. A., Lee, A. F., & Karthikeyan, S. (2017). Cobalt promoted TiO_2/GO for the photocatalytic degradation of oxytetracycline and Congo Red. *Applied Catalysis B: Environmental*. **201**, 159-168. doi: 10.1016/j.apcatb.2016.08.022.

Junjiao, C., Huang, Y., Li, C., Chen, X., & Zhang, X. (2015). Synthesis of NiO@MnO_2 core/shell nanocomposites for supercapacitor application. *Applied Surface Science*. **360**, 534-539. doi: 10.1016/j.apsusc.2015.10.187.

Kadam, S. L., Mane, S. M., Tirmali, P. M., & Kulkarni, S. B. (2018a). Electrochemical synthesis of flower like Mn-Co mixed metal oxides as electrode material for supercapacitor application. *Current Applied Physics*. **18**(4), 397-404. doi: 10.1016/j.cap.2018.01.019.

Kadam, S. L., Mane, S. M., Tirmali, P. M., & Kulkarni, S. B. (2018b). Electrochemical synthesis of flower like Mn-Co mixed metal oxides as electrode material for supercapacitor application. *Current applied Physics*. **18**(4), doi: 10.1016/j.cap.2018.01.019.

Kahimbi, H., Hong, S. B., Yang, M., & Choi, B. G. (2017). Simultaneous synthesis of NiO/reduced graphene oxide composites by ball milling using bulk Ni and graphite oxide for supercapacitor applications. *Journal of Electroanalytical Chemistry*. **786**, 14-19. doi: 10.1016/j.jelechem.2017.01.013.

Kannan, V., Choi, J., Park, H., & Kim, H. (2018). Ultrahigh supercapacitance in cobalt oxide nanorod film grown by oblique angle deposition technique. *Current Applied Physics*. **18**(11), 1399-1402. doi: 10.1016/j.cap.2018.08.004.

Karnan, M., Subramani, K., Srividhya, P. K., & Sathish, M. (2017). Electrochemical Studies on Corncob Derived Activated Porous Carbon for Supercapacitors Application in Aqueous and Non-aqueous Electrolytes. *Electrochimica Acta*. **228**, 586-596. doi: 10.1016/j.electacta.2017.01.095.

Karthik, N., Edison, T. I., Sethuraman, M. G., & Lee, Y. R. (2017). Sonochemical fabrication of petal array-like copper/nickel oxide composite foam as a pseudocapacitive material

for energy storage. *Applied Surface Science*. **396**, 1245-1250. doi: 10.1016/j.apsusc.2016.11.123.

Karthikeyan, K., Kalpana, D., & Renganathan, N. (2009). Synthesis and characterization of $ZnCo_2O_4$ nanomaterial for symmetric supercapacitor applications. *Ionics*. **15**(1), 107-110. doi: doi.org/10.1007/s11581-008-0227-y.

Kasprzak, D., Stępniak, I., & Galiński, M. (2018). Acetate- and lactate-based ionic liquids: Synthesis, characterisation and electrochemical properties. *Journal of Molecular Liquids*. **264**, 233-241. doi: 10.1016/j.molliq.2018.05.059.

Kim, M., Choi, J., Oh, I., & Kim, J. (2016). Design and synthesis of ternary Co_3O_4/carbon coated TiO_2 hybrid nanocomposites for asymmetric supercapacitors. *Physical Chemistry Chemical Physics*. **18**(29), 19696-19704.

Kim, T. H., Veerasubramani, G. K., & Kim, S. J. (2018). Hierarchical porous flower-like nickel cobaltite nanosheets as a binder-less electrode for supercapacitor application with ultra-high capacitance. *Journal of Industrial and Engineering Chemistry*. **61**, 181-187. doi: 10.1016/j.jiec.2017.12.015.

Kim, T. W., & Park, S. J. (2017). Synthesis of reduced graphene oxide/thorn-like titanium dioxide nanofiber aerogels with enhanced electrochemical performance for supercapacitor. *Journal of Colloid and Interface Science*. **486**, 287-295. doi: 10.1016/j.jcis.2016.10.007.

Kong, S., Cheng, K., Gao, Y., Ouyang, T., Ye, K., Wang, G., & Cao, D. (2016). A novel three-dimensional manganese dioxide electrode for high performance supercapacitors. *Journal of Power Sources*. **308**, 141-148. doi: 10.1016/j.jpowsour.2016.01.076.

Kumar , N., Yu, C., Lu, Y. H., & Tseng, T. Y. (2015). Fabrication of carbon nanotube/cobalt oxide nanocomposites via electrophoretic deposition for supercapacitor electrodes. *Journal of Materials Science*. **51**(5), 2320-2329. doi: 10.1007/s10853-015-9540-9.

Kumar, S., Gurmeet, U., Raj, S., & Sharma, K. (2015). Co_3O_4@Reduced Graphene Oxide Nanoribbon for high performance Asymmetric Supercapacitor. *Electrochimica Acta*. **169**, 276-282. doi: 10.1016/j.electacta.2015.03.141.

Lai, F., Miao, Y., Zuo, L., Zhang, Y., & Liu, T. (2016). Carbon Aerogels Derived from Bacterial Cellulose/Polyimide Composites as Versatile Adsorbents and Supercapacitor Electrodes. *Asian Chemical Editorial Society*. **2**(3), 212-219. doi: 10.1002/cnma.201500210.

Lebedeva, M., Ayupov, A., Yeletsky, P., & Parmon, V. (2018). Rice Husk Derived Activated Carbon/Polyaniline Composites As Active Materials For Supercapacitors. *International Journal of Electrochemical Science*. **13**(4), 3674-3690.

Lee, C., Kim, S. K., Choi, J., Chang, H., & Jang, H. D. (2018). Electrochemical performances of iron-cobalt oxides nanoparticles loaded crumpled graphene for supercapacitor. *Journal of Alloys and Compounds*. **735**, 2030-2037. doi: 10.1016/j.jallcom.2017.11.393.

Lei, W., He, P., Wang, Y., Zhang, X., Xia, A., & Dong, F. (2014). Solvothermal preparation of microspherical shaped cobalt–manganese oxide as electrode materials for supercapacitors. *Composites Science and Technology*. 10.1016/j.compscitech.2014.07.019, doi: 10.1016/j.compscitech.2014.07.019.

Lei, X., Shi, Z., Wang, X., Wang, T., Ai, J., Shi, P., . . . Yang, W. (2018). Solvothermal synthesis of pompon-like nickel-cobalt hydroxide/graphene oxide composite for high-performance supercapacitor application. *Colloids and Surfaces* **549**, 76-85. doi: 10.1016/j.colsurfa.2018.04.011.

Li, K., Shi, D., Cai, Z., Zhang, G., Huang, Q., Liu, D., & Yang, C. (2015). Studies on the equivalent serial resistance of carbon supercapacitor. *Electrochimica Acta*. **174**, 596-600. doi: 10.1016/j.electacta.2015.06.008.

Li, L., Liu, X., Liu, C., Wan, H., Zhang, J., Liang, P., . . . Wang, H. (2018a). Ultra-long life nickel nanowires@nickel-cobalt hydroxide nanoarrays composite pseudocapacitive

electrode: Construction and activation mechanism. *Electrochimica Acta*. **259**, 303-312. doi: 10.1016/j.electacta.2017.10.190.

Li, M., ElKady, M. F., Hwang, J. Y., Kowal, M. D., Marsh, K., Wang, H., . . . Kaner, R. B. (2018b). Embedding hollow Co_3O_4 nanoboxes into a three-dimensional macroporous graphene framework for high-performance energy storage devices. *Nano Research*. **11**(5), 2836-2846. doi: 10.1007/s12274-017-1914-7.

Lin, C. (1998). Characterization of Sol-Gel-Derived Cobalt Oxide Xerogels as Electrochemical Capacitors. *Journal of the Electrochemical Society*. **145**(12), 4097. doi: 10.1149/1.1838920.

Linfeng, Z., Shen, F., Smith, R. L., & hua, X. (2016). High-Performance Supercapacitor Electrode Materials from Chitosan via Hydrothermal Carbonization and Potassium Hydroxide Activation. *Energy Technology*. **4**, 1 – 10. doi: 10.1002/ente.201600337.

Lintong, H., Junxian, H., Ying, M., Huiqiao, L., & Tianyou, Z. (2016). Multi-heteroatom self-doped porous carbon derived from swim bladders for large capacitance supercapacitors. *Royal Society of Chemistry*. **4**(39), 15006-15014. doi: 10.1039/C6TA06337C.

Liu, M., Shi, M., Lu, W., Zhu, D., Li, L., & Gan, L. (2017a). Core–shell reduced graphene oxide/MnO_x@carbon hollow nanospheres for high performance supercapacitor electrodes. *Chemical Engineering Journal*. **313**, 518-526. doi: 10.1016/j.cej.2016.12.091.

Liu, T., Ding, J., Su, Z., & Wei, G. (2017b). Porous two-dimensional materials for energy applications: Innovations and challenges. *Materials Today Energy*. **6**, 79-95. doi: 10.1016/j.mtener.2017.08.006.

Liu, Y., Chen, T., Lu, T., Sun, Z., Chua, D. H., & Pan, L. (2015). Nitrogen-doped porous carbon spheres for highly efficient capacitive deionization. *Electrochimica Acta*. **158**, 403-409. doi: 10.1016/j.electacta.2015.01.179.

Long, C., Jiang, L., Wu, X., Jiang, Y., Yang, D., Wang, C., . . . Fan, Z. (2015). Facile synthesis of functionalized porous carbon with three-dimensional interconnected pore structure for high volumetric performance supercapacitors. *Carbon*. **93**, 412-420. doi: 10.1016/j.carbon.2015.05.040.

Ma, W., Chen, S., Yang, S., Chen, W., Weng, W., Cheng, Y., & Zhu, M. (2017). Flexible all-solid-state asymmetric supercapacitor based on transition metal oxide nanorods/reduced graphene oxide hybrid fibers with high energy density. *Carbon*. **113**, 151-158. doi: 10.1016/j.carbon.2016.11.051.

Meng, C., Gall, O. Z., & Irazoqui, P. P. (2013). A flexible super-capacitive solid-state power supply for miniature implantable medical devices. *Biomedical Microdevices*. **15**(6), 973-983. doi: 10.1007/s10544-013-9789-1.

Miao, Y., Yan, J., Huang, Y., Fan, W., & Liu, T. (2015). Electrospun polymer nanofiber membrane electrodes and an electrolyte for highly flexible and foldable all-solid-state supercapacitors. *RSC Advances*. **5**(33), 26189-26196. doi: 10.1039/C5RA00138B.

Mondal, A. K., Kretschmer, K., Zhao, Y., Liu, H., Wang, C., Sun, B., & Wang, G. (2017). Nitrogen-Doped Porous Carbon Nanosheets from Eco-Friendly Eucalyptus Leaves as High Performance Electrode Materials for Supercapacitors and Lithium Ion Batteries. *Chemistry*. **23**(15), 3683-3690. doi: 10.1002/chem.201605019.

Moreno, G., Ibañez, J., Rojo, J. M., & Kunowsky, M. (2017). Activated Carbon Fiber Monoliths as Supercapacitor Electrodes. *Advances in Materials Science and Engineering*. **2017**, 1-8. doi: 10.1155/2017/3625414.

Numan, A., Duraisamy, N., Saiha Omar, F., Mahipal, Y. K., Ramesh, K., & Ramesh, S. (2016). Enhanced electrochemical performance of cobalt oxide nanocube intercalated reduced graphene oxide for supercapacitor application. *RSC Advances*. **6**(41), 34894-34902. doi: 10.1039/c6ra00160b.

Nwanya, A. C., Obi, D., Osuji, R. U., Bucher, R., Maaza, M., & Ezema, F. I. (2017). Simple chemical route for nanorod-like cobalt oxide films for electrochemical energy storage

applications. *Journal of Solid State Electrochemistry*. **21**(9), 2567-2576. doi: 10.1007/s10008-017-3520-8.

Oschatz, M., Boukhalfa, S., Nickel, W., Hofmann, J. P., Fischer, C., Yushin, G., & Kaskel, S. (2017). Carbide-derived carbon aerogels with tunable pore structure as versatile electrode material in high power supercapacitors. *Carbon*. **113**, 283-291. doi: 10.1016/j.carbon.2016.11.050.

Osti, N. C., Gallegos, A., Dyatkin, B., Wu, J., Gogotsi, Y., & Mamontov, E. (2018). Mixed Ionic Liquid Improves Electrolyte Dynamics in Supercapacitors. *American Chemical Society*. **122**(19), 10476-10481. doi: 10.1021/acs.jpcc.8b02521.

Paraknowitsch, J. P., & Thomas, A. (2013). Doping carbons beyond nitrogen: an overview of advanced heteroatom doped carbons with boron, sulphur and phosphorus for energy applications. *Energy and Environmental Science*. **6**, 2839-2855. doi: 10.1039/c3ee41444b.

Patil, J. V., Mali, S. S., Shaikh, J. S., Bhat, T. S., Hong, C. K., Kim, J. H., & Patil, P. S. (2018). Hydrothermally grown 3D hierarchical TiO_2 based on electrochemically anodized 1D TiO_2 nanostructure for supercapacitor. *Applied Physics A*. **124**(9), doi: 10.1007/s00339-018-1937-2.

Pham, V. H., Nguyen, T., Tong, X., Rajagopalan, B., & Jin Suk Chung, J. H. D. (2018). Hydrogenated TiO_2@reduced graphene oxide sandwich-like nanosheets for high voltage supercapacitor applications. *Carbon*. **126**, 135-144. doi: 10.1016/j.carbon.2017.10.026.

Rakhi, R. B., Beaujuge, D. H. N. P., & Alshareef, H. N. (2016). Supercapacitors based on two dimensional VO_2 nanosheet electrodes in organic gel electrolyte. *Electrochimica Acta*. **220**, 601-608. doi: 10.1016/j.electacta.2016.10.109.

Rakhi, R. B., & Lekshmi, M. L. (2017). Reduced graphene oxide based ternary nanocomposite cathodes for high-performance aqueous asymmetric supercapacitors. *Electrochimica Acta*. **231**, 539-548. doi: 10.1016/j.electacta.2017.02.095.

Ramesh, S., Khandelwal, S., Rhee, K. Y., & Hui, D. (2018). Synergistic effect of reduced graphene oxide, CNT and metal oxides on cellulose matrix for supercapacitor applications. *Composites Part B: Engineering*. **138**, 45-54. doi: 10.1016/j.compositesb.2017.11.024.

Raymundo, E., Kierzek, K., Machnikowski, J., & Be´guin, F. (2006). Relationship between the nanoporous texture of activated carbons and their capacitance properties in different electrolytes. *Carbon*. **44**(12), 2498-2507. doi: 10.1016/j.carbon.2006.05.022.

Rose, A., Guru Prasad, K., Sakthivel, T., Gunasekaran, V., Maiyalagan, T., & Vijayakumar, T. (2018). Electrochemical analysis of Graphene Oxide/Polyaniline/Polyvinyl alcohol composite nanofibers for supercapacitor applications. *Applied Surface Science*. **449**, 551-557. doi: 10.1016/j.apsusc.2018.02.224.

Sahoo, S., & Satpati, A. K. (2017). Electrochemical capacitance properties of cobalt oxide entangled over MWCNT and cobalt oxide AC composites. *Journal of Electroanalytical Chemistry*. **801**, 416-424. doi: 10.1016/j.jelechem.2017.08.022.

Salanne, M. (2017). Ionic Liquids for Supercapacitor Applications. *Current Chemistry Collections*. **375(**3), 63. doi: 10.1007/s41061-017-0150-7.

Salunkhe, R. R., Lin, J., Malgras, V., Dou, S. X., Kim, J. H., & Yamauchi, Y. (2015). Large-scale synthesis of coaxial carbon nanotube/$Ni(OH)_2$ composites for asymmetric supercapacitor application. *Nano Energy*. **11**, 211-218. doi: 10.1016/j.nanoen.2014.09.030.

Seo, M., & Park, S. (2010). Effect of nanosize titanium oxide on electrochemical characteristics of activated carbon electrodes. *Current Applied Physics*. **10**(2), 391-394. doi: 10.1016/j.cap.2009.06.032.

Shown, I., Ganguly, A., Chen, L., & Chen, K. (2015). Conducting polymer-based flexible supercapacitor. *Energy Science and Engineering*. **3**(1), 2-26. doi: 10.1002/ese3.50.

Simon, J. A., Vickraman, P., & Reddy, B. J. (2018). Synthesis and characterization of high porous carbon sphere@nickel oxide core-shell nanocomposite for supercapacitor

applications. *Journal of Electroanalytical Chemistry*. **823**, 342-349. doi: 10.1016/j.jelechem.2018.06.009.

Sk, M. M., Yue, C. Y., Ghosh, K., & Jena, R. K. (2016). Review on advances in porous nanostructured nickel oxides and their composite electrodes for high-performance supercapacitors. *Journal of Power Sources*. **308**, 121-140. doi: 10.1016/j.jpowsour.2016.01.056.

Stankovich, S., Dikin, D. A., Piner, R. D., Kohlhaas, K. A., Kleinhammes, A., Jia, Y., . . . Ruoff, R. S. (2007). Synthesis of graphene-based nanosheets via chemical reduction of exfoliated graphite oxide. *Carbon*. **45**, 1558–1565. doi: 10.1016/j.carbon.2007.02.034.

Su, X., Chen, J., Zheng, G., Yang, J., Guan, X., Liu, P., & Zheng, C. (2018). Three-dimensional porous activated carbon derived from loofah sponge biomass for supercapacitor applications. *Applied Surface Science*. **436**, 327-336. doi: 10.1016/j.apsusc.2017.11.249.

Tajik, S., Dubal, D., Gomez, P., Yadegari, A., Rashidi, A., Nasernejad, B., . . . Asiri, A. M. (2017). Nanostructured mixed transition metal oxides for high performance asymmetric supercapacitors: Facile synthetic strategy. *International Journal of Hydrogen Energy*. **42**(17), 12384-12395. doi: 10.1016/j.ijhydene.2017.03.117.

Tao, Y., Xie, X., Lv, W., Tang, M., Kong, D., Huang, Z., . . . Yang, H. (2013). Towards ultrahigh volumetric capacitance: graphene derived highly dense but porous carbons for supercapacitors. *Scientific reports*. **3**, 2975. doi: 10.1038/srep02975.

Thangavela, R., Kannanb, A. G., Ponrajb, R., Thangavelc, V., Kimb, D., & Leea, Y. (2018). High-energy green supercapacitor driven by ionic liquid electrolytes as an ultra-high stable next-generation energy storage device. *Journal of Power Sources*. **383**, 102–109. doi: 10.1016/j.jpowsour.2018.02.037.

To, J. W., Chen, Z., Yao, H., He, J., Kim, K., Chou, H. H., . . . Bao, Z. (2015). Ultrahigh Surface Area Three-Dimensional Porous Graphitic Carbon from Conjugated

Polymeric Molecular Framework. *ACS Central Science*. **1**(2), 68-76. doi: 10.1021/acscentsci.5b00149.

Veeramani, V., Madhu, R., Chen, S., Sivakumar, M., Hung, C., Miyamoto, N., & Liu, S. (2017a). $NiCo_2O_4$-decorated porous carbon nanosheets for high-performance supercapacitors. *Electrochimica Acta*. **247**(17), 288-295. doi: 10.1016/j.electacta.2017.06.171.

Veeramani, V., Madhu, R., Chen, S., Sivakumar, M., Hung, C., Miyamoto, N., & Liu, S. (2017b). $NiCo_2O_4$-decorated porous carbon nanosheets for high-performance supercapacitors. *Electrochimica Acta*. **247**, 288-295. doi: 10.1016/j.electacta.2017.06.171.

Vidhyadharan, B., Zain, N. K. M., Misnon, I. I., Aziz, R. A., Ismail, J., Yusoff, M. M., & Jose, R. (2014). High performance supercapacitor electrodes from electrospun nickel oxide nanowires. *Journal of Alloys and Compounds*. **610**, 143-150. doi: 10.1016/j.jallcom.2014.04.211.

Vijayabala, V., Senthilkumar, N., Nehru, K., & Karvembu, R. (2017). Hydrothermal synthesis and characterization of ruthenium oxide nanosheets using polymer additive for supercapacitor applications. *Journal of Materials Science: Materials in Electronics*. **29**(1), 323-330. doi: 10.1007/s10854-017-7919-x.

Wan, L., Shamsaei, E., Easton, C. D., Yu, D., Liang, Y., Chen, X., . . . Wang, H. (2017). ZIF-8 derived nitrogen-doped porous carbon/carbon nanotube composite for high-performance supercapacitor. *Carbon*. **121**, 330-336. doi: 10.1016/j.carbon.2017.06.017.

Wang, Chen, S., Li, D., Sun, S., Peng, Z., Komarneni, S., & Yang, D. (2017a). Direct Interfacial Growth of MnO_2 Nanostructure on Hierarchically Porous Carbon for High-Performance Asymmetric Supercapacitors. *American Chemical Society*. **6**(1), 633–641. doi: 10.1021/.

Wang, H., Huang, X., Lin, J., Cui, J., Chen, Y., Zhu, C., . . . Yu, P. (2017b). High-quality monolayer superconductor $NbSe_2$ grown by chemical vapour deposition. *Nature Communications*. **8**(1), 394. doi: 10.1038/s41467-017-00427-5.

Wang, J., & Kaskel, S. (2012). KOH activation of carbon-based materials for energy storage. *Journal of Materials Chemistry*. **22**, 23710-23725 doi: 10.1039/C2JM34066F.

Wang, M., & Zhang, X. (2017). Three-Dimensional Co_3O_4@$NiCo_2S_4$ Core/Shell Nanoflower Array with Enhanced Electrochemical Performance. *Chemistry Select*. **2**(29), 9537-9545. doi: 10.1002/slct.201700746.

Wang, W., Hu, Z., Chang, Q., Chen, L., Wu, Y., Zhang, Y., & Yang, Y. (2011). Design and synthesis of $NiCo_2O_4$–reduced graphene oxide composites for high performance supercapacitors. *Journal of Materials Chemistry*. **21**(28), 10504. doi: 10.1039/c1jm10758e.

Wang, X., Han, X., Lim, M., Singh, N., Gan, C. L., Jan, M., & Lee, P. S. (2012). Nickel Cobalt Oxide-Single Wall Carbon Nanotube Composite Material for Superior Cycling Stability and High-Performance Supercapacitor Application. *The Journal of Physical Chemistry C*. **116**(23), 12448-12454. doi: 10.1021/jp3028353.

Wang, Y., He, P., Lei, W., Dong, F., & Zhang, T. (2014). Novel $FeMoO_4$/graphene composites based electrode materials for supercapacitors. *Composites Science and Technology*. **103**, 16-21. doi: 10.1016/j.compscitech.2014.08.009.

Wang , Y., Tang, S., Vongehr, S., Syed, J. A., Wang, X., & Meng, X. (2016). High-Performance Flexible Solid-State Carbon Cloth Supercapacitors Based on Highly Processible N-Graphene Doped Polyacrylic Acid/Polyaniline Composites. *Scientific reports*. **6**, 12883. doi: 10.1038/srep12883.

Wanga, J. Y., Kadya, M. F., Lia, M., Lina, C., Kowala, M., Hana, X., & Kanera, R. B. (2017). Boosting the capacitance and voltage of aqueous supercapacitors viaredox charge contribution from both electrode and electrolyte. *Nano Today*. **15**, 15-25. doi: 10.1016/j.nantod.2017.06.009.

Wei, H., Wang, J., Yu, L., Zhang, Y., Hou, D., & Li, T. (2017). Hydrothermal preparation of nickel-manganese oxide with microsphere structure grown on Ni foam and supercapacitive performance. *Materials Letters*. **187**, 11-14. doi: 10.1016/j.matlet.2016.10.034.

Wu, C., Ma, J., & Lu, C. (2012). Synthesis and characterization of nickel–manganese oxide via the hydrothermal route for electrochemical capacitors. *Current Applied Physics*. **12**(4), 1190-1194.

Wu, S., Hui, K. S., & Hui, K. N. (2018). Carbon nanotube@manganese oxide nanosheet core-shell structure encapsulated within reduced graphene oxide film for flexible all-solid-state asymmetric supercapacitors. *Carbon*. **132**, 776-784. doi: 10.1016/j.carbon.2017.12.051.

Xi, S., Zhu, Y., Yang, Y., Jiang, S., & Tang, Z. (2017). Facile Synthesis of Free-Standing NiO/MnO_2 Core-Shell Nanoflakes on Carbon Cloth for Flexible Supercapacitors. *Nanoscale Research Letters*. **12**(1), 171. doi: doi.org/10.1186/s11671-017-1939-6.

Xi , Y., Fei, B., Ma, J., Liu, X., Yang, S., Tian, G., & Jiang, Z. (2017). Porous nanoplatelets wrapped carbon aerogel by pyrolysis of regenerated bamboo cellulose aerogels as supercapacitor electrodes. *Carbohydrate Polymers*. **16**(5), 323-329. doi: 10.1016/j.carbpol.2017.10.013.

Xia, S., Jing Ran, C., Guang Ping, Z., Jing He, Y., Xin Xin, G., Pu, L., & Xiu Cheng, Z. (2018). Three-dimensional porous activated carbon derived from loofah sponge biomass for supercapacitor applications. *Applied Surface Science*. **436**, 327-336. doi: 10.1016/j.apsusc.2017.11.249.

Xiao, H., Guo, W., Sun, B., Pei, M., & Zhou, G. (2016). Mesoporous TiO_2 and Co-doped TiO_2 nanotubes/reduced graphene oxide composites as electrodes for supercapacitors. *Electrochimica Acta*. **190**, 104-117. doi: 10.1016/j.electacta.2016.01.040.

Xiao, Q., & Zhou, X. (2013). The study of multiwalled carbon nanotube deposited with conducting polymer for supercapacitor. *Electrochimica Acta*. **48**(5), 575-580. doi: 10.1016/S0013-4686(02)00727-2.

Xie, J., Wu, F., Chen, C., Zhang, C., Wan, L., Wang, J., . . . Sun, H. (2013). A novel asymmetric supercapacitor with an activated carbon cathode and a reduced graphene oxide–cobalt oxide nanocomposite anode. *Journal of Power Sources*. **242**, 148-156. doi: 10.1016/j.jpowsour.2013.05.081.

Xie , Q., Zhou, S., Zheng, A., Xie, C., Yin, C., Wu, S., . . . Zhao, P. (2016). Sandwich-like nitrogen-enriched porous carbon/graphene composites as electrodes for aqueous symmetric supercapacitors with high energy density. *Electrochimica Acta*. **189**, 22-31. doi: 10.1016/j.electacta.2015.12.087.

Xu, P., Wang, G., Miao, C., Cheng, K., Ye, K., Zhu, K., . . . Zhang, X. (2018). Controllable one-pot synthesis of emerging β-Cu2Se nanowire freely standing on nickel foam for high electrochemical energy storage performance. *Applied Surface Science*. **463**, 82-90. doi: 10.1016/j.apsusc.2018.08.147.

Xu , Q., Wei, C., Fan, L., Rao, W., Xu, W., Liang, H., & Xu, J. (2017). Polypyrrole/titania-coated cotton fabrics for flexible supercapacitor electrodes. *Applied Surface Science*. **460**, 84-91. doi: 10.1016/j.apsusc.2017.12.128.

Yadav, A. A., Hunge, Y. M., & Kulkarni, S. B. (2018). Chemical synthesis of Co_3O_4 nanowires for symmetric supercapacitor device. *Journal of Materials Science: Materials in Electronics*. **29**(19), 16401–16409. doi: 10.1007/s10854-018-9731-7.

Yang, Y., He, L., Tang, C., Hu, P., Hong, X., Yan, M., . . . Mai, L. (2016). Improved conductivity and capacitance of interdigital carbon microelectrodes through integration with carbon nanotubes for micro-supercapacitors. *Nano Research*. **9**(8), 2510-2519. doi: 10.1007/s12274-016-1137-3.

Yating, H., Wu, Y., & Wang, J. (2018). Manganese-Oxide-Based Electrode Materials for Energy Storage Applications: How Close Are We to the Theoretical Capacitance? *Advanced Materials*. **9**, 345-351. doi: 10.1002/adma.201802569.

Ying, W., Zhang, M., Li, Y., Ma, T., Liu, H., Pan, D., . . . Wang, A. (2018). Rational design 3D nitrogen doped graphene supported spatial crosslinked Co_3O_4@$NiCo_2O_4$ on nickel

foam for binder-free supercapacitor electrodes. *Electrochimica Acta*. **290**, 12-20. doi: 10.1016/j.electacta.2018.09.060.

Yong, W., & Xiao, Z. (2004). Preparation and electrochemical capacitance of RuO_2/TiO_2 nanotubes composites. *Electrochimica Acta*. **49**(12), 1957-1962. doi: 10.1016/j.electacta.2003.12.023.

Yu, M., Han, Y., Li, J., & Wang, L. (2017). CO_2-activated porous carbon derived from cattail biomass for removal of malachite green dye and application as supercapacitors. *Chemical Engineering Journal*. **317**, 493-502. doi: 10.1016/j.cej.2017.02.105.

Yu, M., Han, Y., Li, Y., Li, J., & Wang, L. (2018). Polypyrrole-anchored cattail biomass-derived carbon aerogels for high performance binder-free supercapacitors. *Carbohydrate Polymers*. **199**, 555-562. doi: 10.1016/j.carbpol.2018.04.058.

Zhang, Xie, Y., Zhao, M., Pentecost, A. E., Ling, Z., Wang, J., . . . Qiao, W. (2014a). Enhanced electrochemical performance of hydrous RuO_2/mesoporous carbon nanocomposites via nitrogen doping. *Applied Material Interfaces*. **6**(12), 9751-9759. doi: 10.1021/am502173x.

Zhang, Zhao, Y., Cao, S., Yin, Z., Cheng, L., & Wu, L. (2017a). Design and Synthesis of Hierarchical SiO_2@C/TiO_2 Hollow Spheres for High-Performance Supercapacitors. *Applied Materials and Interfaces*. **9**(35), 29982-29991. doi: 10.1021/acsami.7b08776.

Zhang, C., Lei, C., Cen, C., Tang, S., Deng, M., Li, Y., & Du, Y. (2018a). Interface polarization matters: Enhancing supercapacitor performance of spinel $NiCo_2O_4$ nanowires by reduced graphene oxide coating. *Electrochimica Acta*. **260**, 814-822. doi: 10.1016/j.electacta.2017.12.044.

Zhang, G., Chen, Y., Chen, Y., & Guo, H. (2018b). Activated biomass carbon made from bamboo as electrode material for supercapacitors. *Materials Research Bulletin*. **102**, 391-398. doi: 10.1016/j.materresbull.2018.03.006.

Zhang, Y., Wang, F., Zhu, H., Zhang, D., & Chen, J. (2017b). Elongated TiO_2 nanotubes directly grown on graphene nanosheets as an efficient material for supercapacitors

and absorbents. *Composites Part A: Applied Science and Manufacturing*. **101**, 297-305. doi: 10.1016/j.compositesa.2017.06.026.

Zhang, Y. Q., Li, L., Shi, S. J., Xiong, Q. Q., Zhao, X. Y., Wang, X. L., . . . Tu, J. P. (2014b). Synthesis of porous Co_3O_4 nanoflake array and its temperature behavior as pseudo-capacitor electrode. *Journal of Power Sources*. **256**, 200-205. doi: 10.1016/j.jpowsour.2014.01.073.

Zhao, C., Shao, X., Zhang, Y., & Qian, X. (2016). Fe_2O_3/RGO/Fe_3O_4 Composite in-situ Grown on Fe Foil for High performance Supercapacitors. *Applied Materials and Interfaces*. **44**(8), 30133-30142. doi: doi.org/10.1021/acsami.6b09594.

Zhao, C., & Zheng, W. (2015). A Review for Aqueous Electrochemical Supercapacitors. *Frontiers in Energy Research*. **3**, 23. doi: 10.3389/fenrg.2015.00023.

Zhao, T., Yang, W., Zhao, X., Peng, X., Hu, J., Tang, C., & Li, T. (2018). Facile preparation of reduced graphene oxide/copper sulfide composite as electrode materials for supercapacitors with high energy density. *Composites Part B: Engineering*. **150**, 60-67. doi: 10.1016/j.compositesb.2018.05.058.

Zhou, H., Peng, Y., Wu, H. B., Sun, F., Yu, H., Liu, F., . . . Lu, Y. (2016). Fluorine-rich nanoporous carbon with enhanced surface affinity in organic electrolyte for high-performance supercapacitors. *Nano Energy*. **21**, 80-89. doi: doi.org/10.1016/j.nanoen.2015.12.016.

Zhou, M., Glushenkov, A. M., Kartachova, O., Li, Y., & Chen, Y. (2015). Titanium Dioxide Nanotube Films for Electrochemical Supercapacitors: Biocompatibility and Operation in an Electrolyte Based on a Physiological Fluid. *Journal of the Electrochemical Society*. **162**(5), 5065-5069. doi: 10.1149/2.0101505jes.

Zhu, G., Yang, J., Liu, Y., Xie, X., Ji, Z., Yin, J., & Shen, X. (2016). Porous Fe-Mn-O nanocomposites: Synthesis and supercapacitor electrode application. *Progress in Natural Science: Materials International*. **26**(3), 264-270. doi: 10.1016/j.pnsc.2016.05.016i.

Zhua, H., Jinga, Y., Pala, M., Liua, Y., Liua, Y., Wanga, J., . . . Zhaoa, D. (2016). Mesoporous TiO_2@N-doped Carbon Composite Nanospheres Synthesized by Direct Carbonization of Surfactants after Sol-gel Process for Superior Lithium Storage. *Royal Society of Chemistry*. **9**, 1539-1546 doi: 10.1039/C6NR08885F.

Zou, Deng, Y., Chen, J., Qian, Y., Yang, Y., Li, Y., & Chen, G. (2018). Hierarchically porous nitrogen-doped carbon derived from the activation of agriculture waste by potassium hydroxide and urea for high-performance supercapacitors. *Journal of Power Sources*. **378**, 579-588. doi: 10.1016/j.jpowsour.2017.12.081.

Zu, G., Shen, J., Zou, L., Wang, F., & Zhang, Y. (2016). Nanocellulose-Derived Highly Porous Carbon Aerogels for Supercapacitors. *Carbon*. **99**, 203-211. doi: 10.1016/j.carbon.2015.11.079.